CMOS SPAD sensors with embedded smartness

Ion Vornicu, Ricardo Carmona-Galán and Ángel Rodríguez-Vázquez

ivornicu@imse-cnm.csic.es

International SPAD-Sensor Workshop; Edinburg, Scotland (UK) June 2020

IMSE -cnm Instituto de Microelectrónica de Sevilla

UNIVERSIDAD DE SEVILLA

CSIC
CONSEJO SUPERIOR DE INVESTIGACIONES CIENTÍFICAS

- **R&D Center ran by University of Seville and the Spanish Council of Research**
  - Part of the Spanish Microelectronic Center
  - Specialized on Mixed-Signal Systems and Smart Sensory Systems
- **Human Resources**
  - About 90 people:
    - US ~60%
    - CSIC ~40%
    - Permanent ~49%
    - Temporary ~51%
    - Women ~26%
    - Men ~74%
- **Laboratory Equipment:**
  - Labs for logical, electrical, functional and thermal characterization of mixed signal, RF and optoelectronic ICs

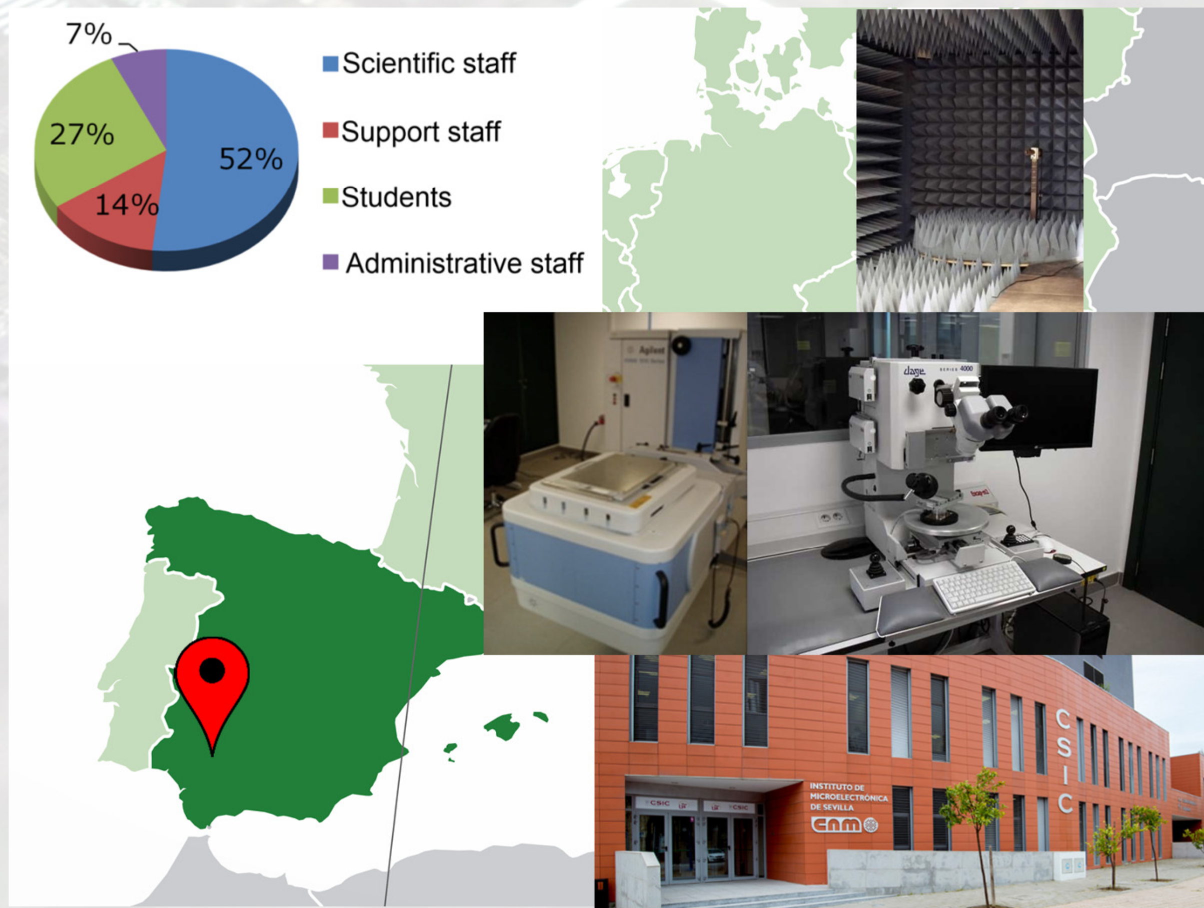

Group on *Intelligent Interface Circuits and Sensory Systems* (I2CASS)

IMSE-CNM

- **Group Head: Prof. Ángel Rodríguez-Vázquez**
- **Scope of the R&D Activities:**
  - **Focus on Complete Smart-Sensory Systems**
    - **Aligned to ITRS and prevalent micro-electronic trends**
    - **Innovation at chip architecture and design levels**
    - **Innovation at system embedding and applications**
  - **Major emphasis on vision sensors and bio-medical recording and stimulation systems**
  - **Balance between academic production and technology transfer**
  - **Several Mixed-signal AFEs in commercial exploitation for high-speed communications and automotive sensors**
  - **Three EBTs emerged from the group; all in operation**

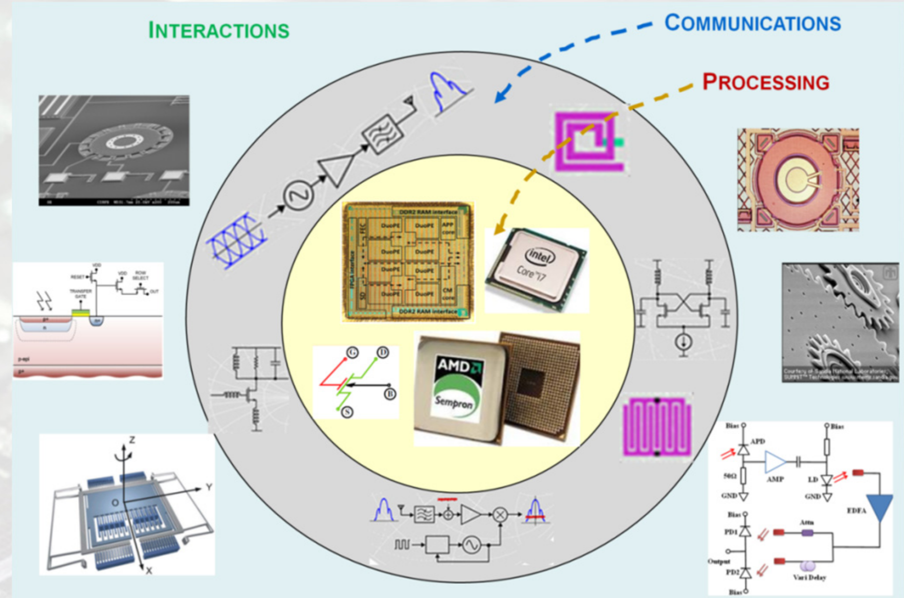

- **Activity of Image and Vision Sensors:**
  - Bio-inspired sensor architectures for high-speed energy-efficient vision systems:
    - Feature-extraction based sensors
  - Event-driven and dynamic vision sensors
  - High-Dynamic range and Low-noise image sensors
  - Vision sensors with Deep Learning at the Edge
  - **SPAD-based imagers and vision sensors**

Outlines

1. LiDAR challenges
2. Active illumination
3. SPAD detectors
4. Noise suppression
5. Low power architecture
6. ToF data processing
7. Conclusions

Outlines

➊ **LiDAR challenges**

➋ Active illumination

➌ SPAD detectors

➍ Noise suppression

➎ Low power architecture

➏ ToF data processing

➐ Conclusions

LiDAR challenges

LiDARs:
- Short range: ×4
- 360 view: ×1
- Long range: ×1

Radars: ×4 (360º view)

Cameras: ×8 (360º view)

Other sensors:
- Ultrasonic: ×8
- GPS/IMU: ×2

March 4, 2020:

https://blog.waymo.com/2020/03/introducing-5th-generation-waymo-driver.html

Flash or Scanning?
- **Range**
- **Eye safety IEC 60825**
- **Laser technology**

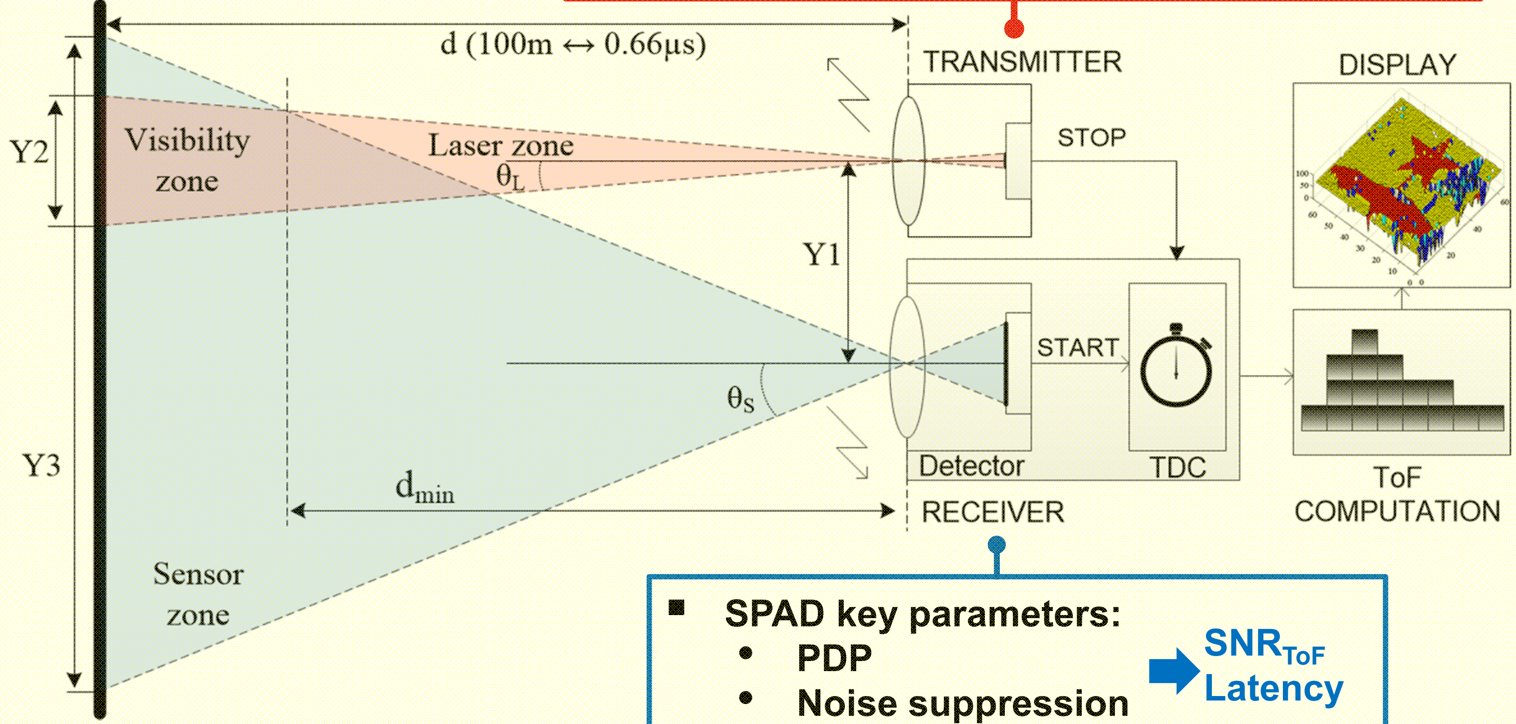

ToF processing
- **Memory size**
- **Latency**

- **SPAD key parameters:**
  - **PDP**
  - **Noise suppression**

  ➡ **SNR$_{ToF}$ Latency**
- **Detector array power consumption**
- **Read out strategy**

Outlines

1. LiDAR challenges
2. **Active illumination**
3. SPAD detectors
4. Noise suppression
5. Low power architecture
6. ToF data processing
7. Conclusions

Active illumination

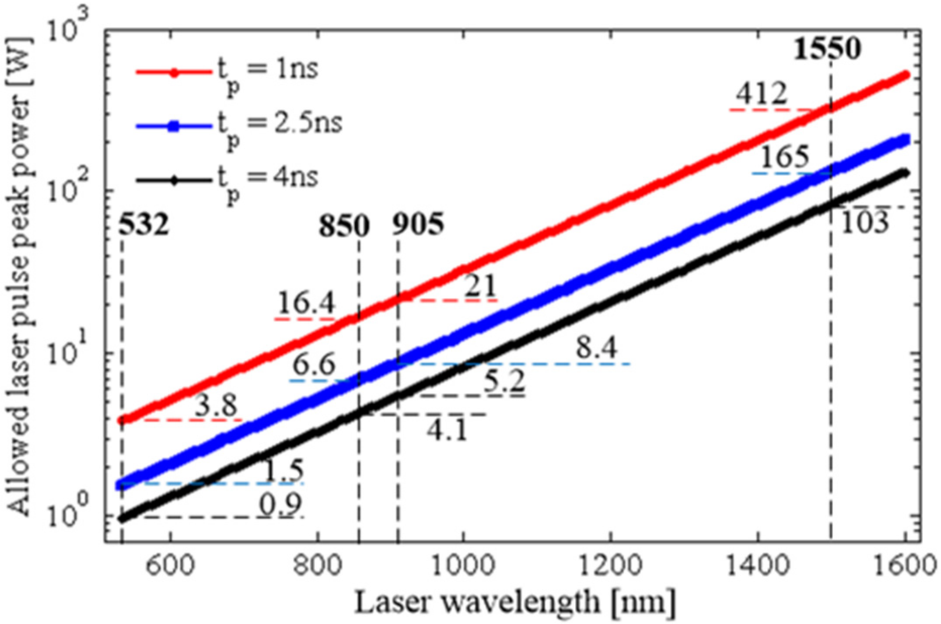

Maximum allowed peak P_{opt} vs. λ; 30s exposure time; iris Φ of 7mm; laser frequency of 10 kHz; IEC 60825-1 (2001))

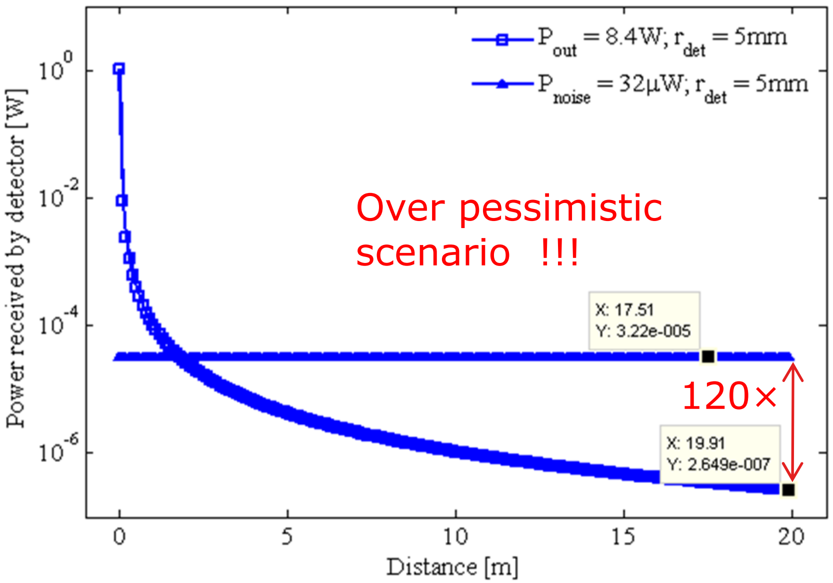

Received power at 905nm; 50% reflectivity

- **Gaussian beam distribution:**

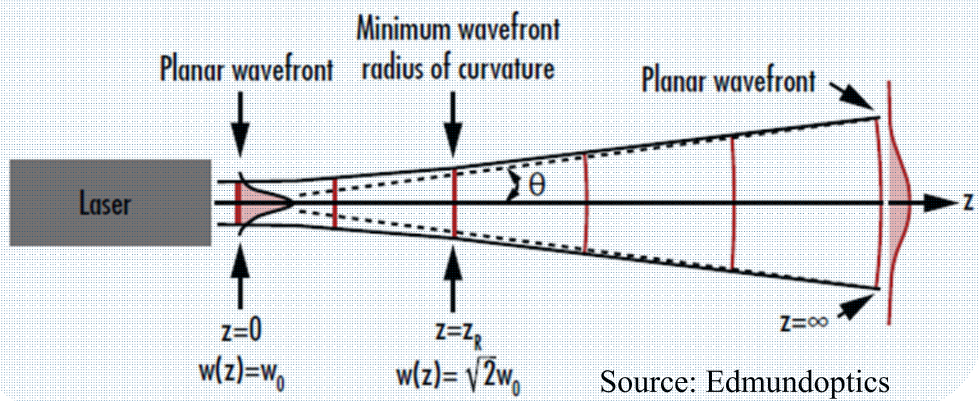

z = 10cm
D = 7mm

- **Extra power budget:**
  - 4× P_{opt} for 850nm
  - 5× P_{opt} for 905nm

Active illumination

Range	Emitter (laser)	Wavelength	3D Imaging
Short: <20m	VCSEL	<1000nm	Flash
Medium: 20-100m	Edge emitting	850nm, 905nm, 940nm, 1550nm	Scanning
Long: >100m	Edge emitting		Scanning

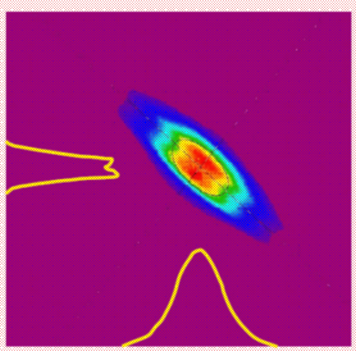

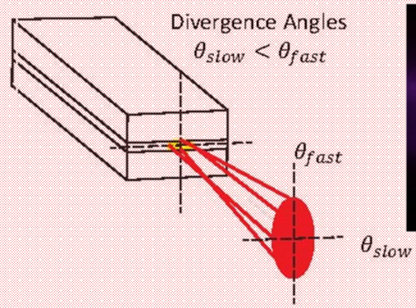

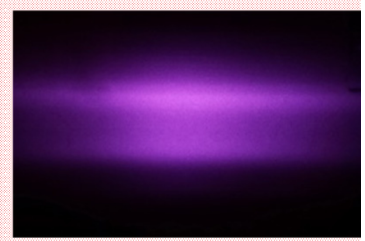

905nm emission (10µm×85µm)

Edge emitting laser emit elliptical beams

Pros:
- **Long range**
- **Higher efficiency**

Cons:
- **Hard to obtain uniform pattern**
- **Limited duty cycle (0.1% without cooling)**

- **Addressable VCSEL (Philips)**

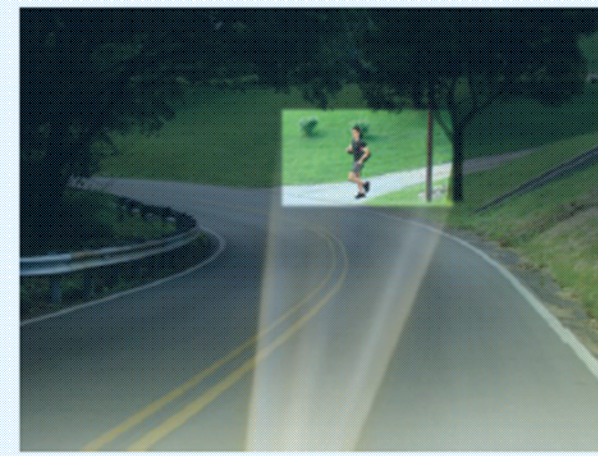

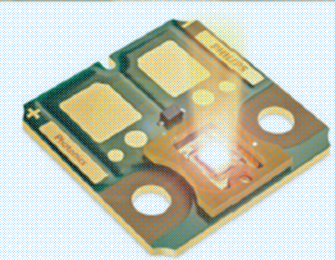

Pros:
- **Lower switching currents**
- **Uniform illumination**

Cons:
- **Lower efficiency**
- **Temperature stability**
- **Smaller output power**

Outlines

SPAD detectors for LiDAR: EQE

$$EQE(\lambda) = \frac{|I_A|}{SPC(\lambda)}$$

$$PDP = QE(\lambda) \cdot P_{tr}$$

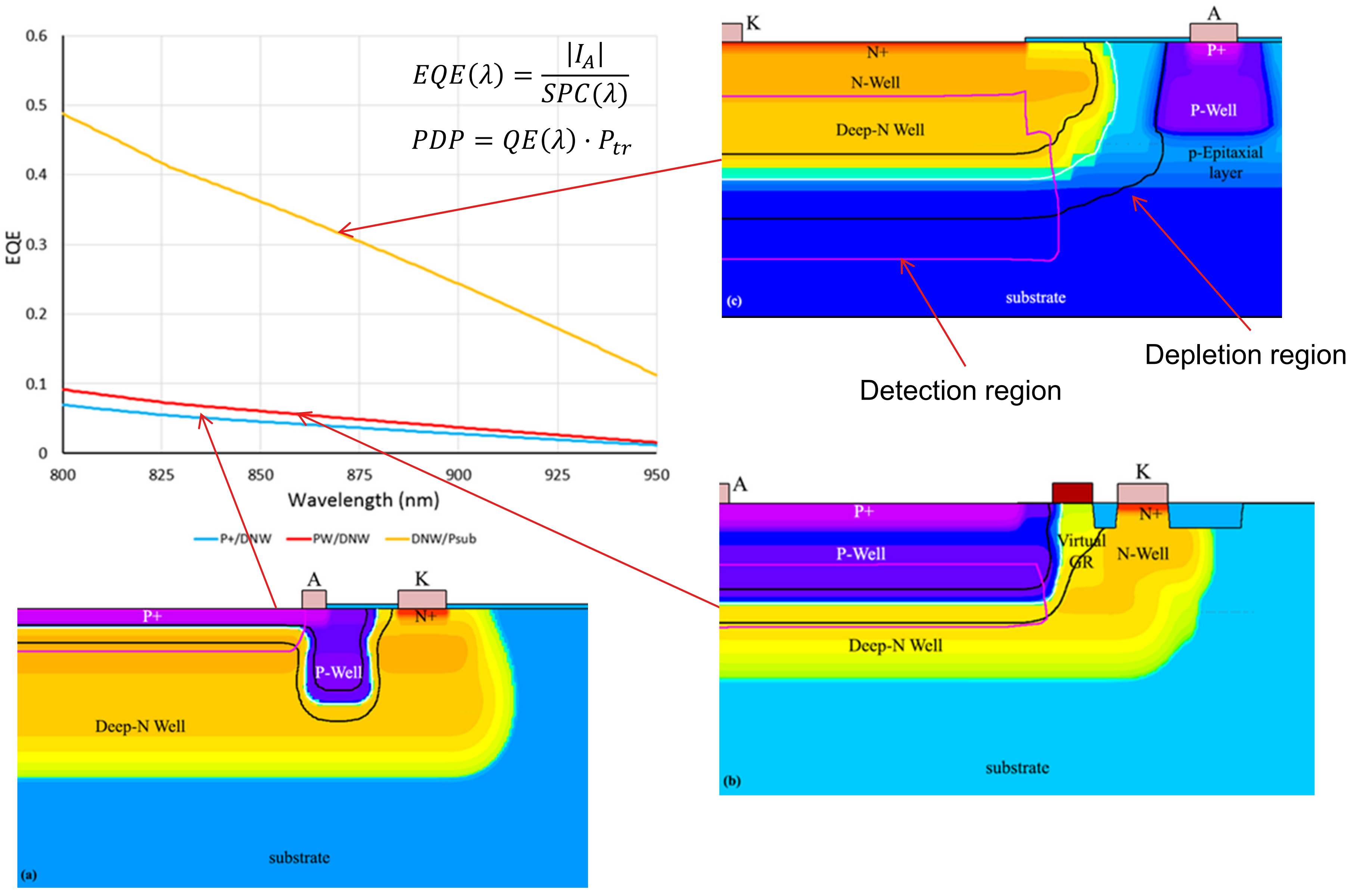

SPAD detectors for LiDAR: Crosstalk (1)

Source of electrical crosstalk:

- Charge carriers generated by light
- Charge carriers generated by avalanche (negligible)

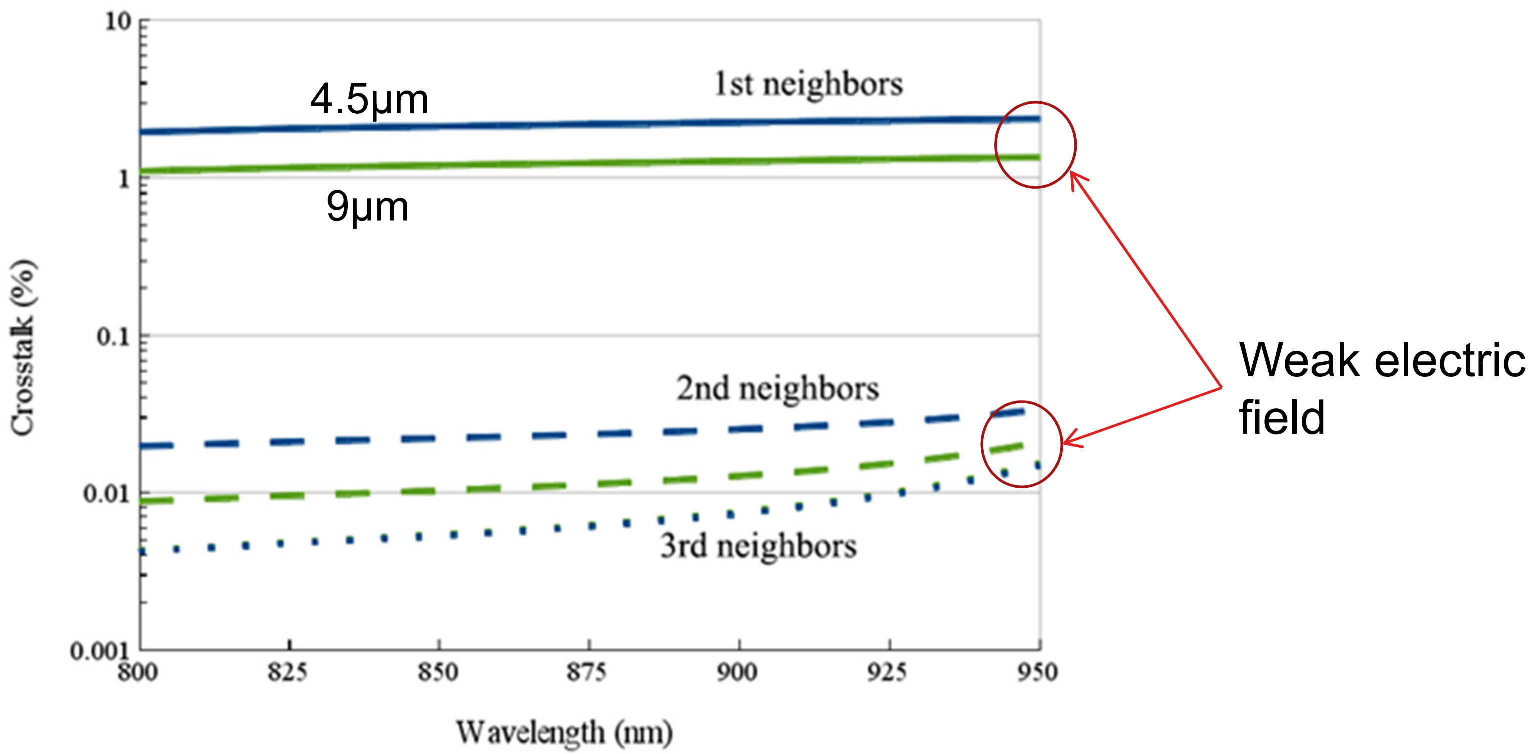

SPAD detectors for LiDAR: Crosstalk (2)

Source of optical crosstalk:

- Radiative recombination

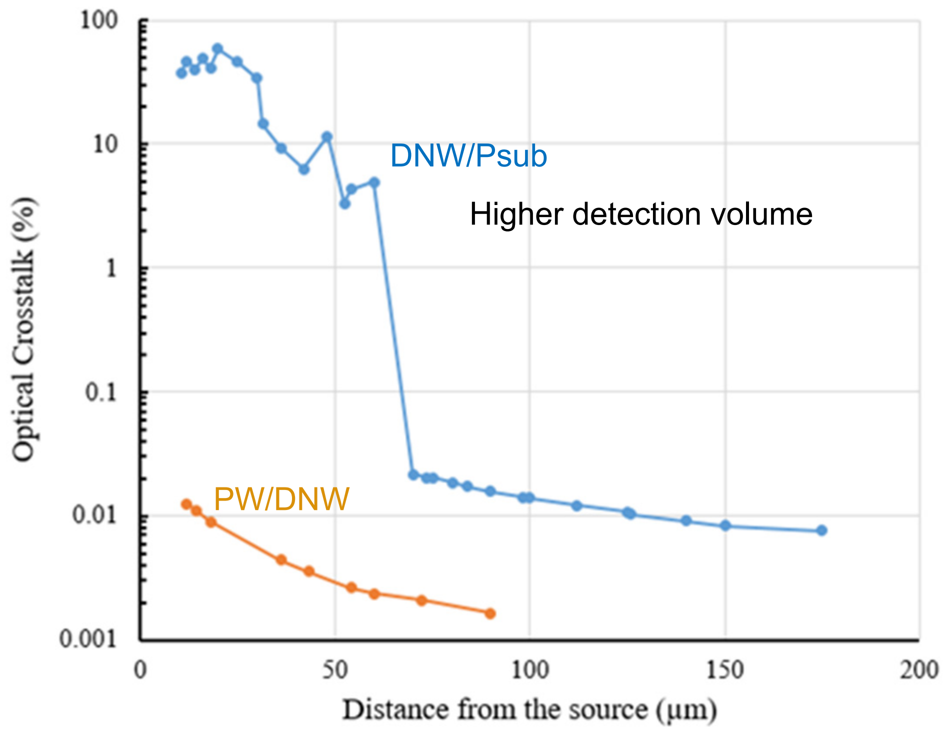

Radiative recombination in PW/DNW

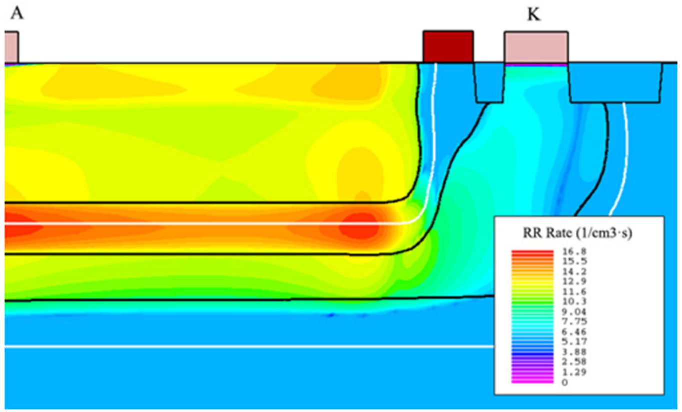

$$RR = B(np - n_i^2); B = 4.73 \cdot 10^{-15}\ \mathrm{cm^3 s^{-1}}$$

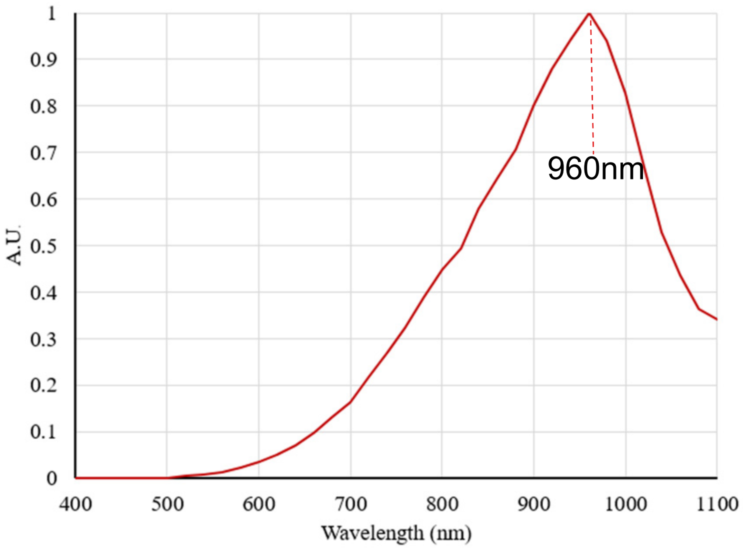

Emission spectrum of avalanche in Si
[Rech, Opt. Exp. 2008]

SPAD detectors for LiDAR: PW/DNW in 110nm CIS

- **PWell/Deep-NWell SPAD junction:**

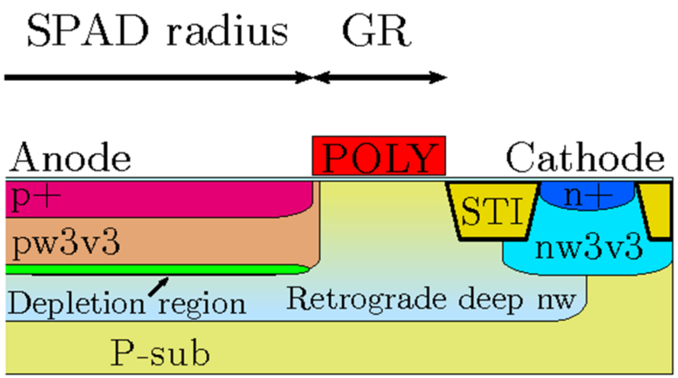

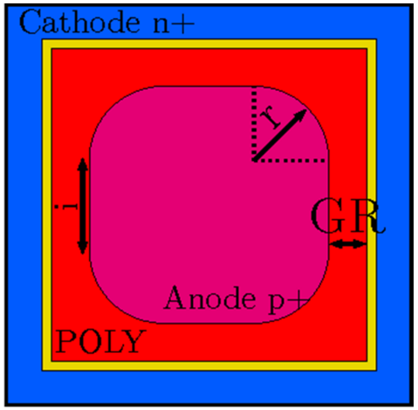

$$A_{SPAD} = \pi r^2 + 4i(i + 2r)$$

- **Schematic of test pixel:**

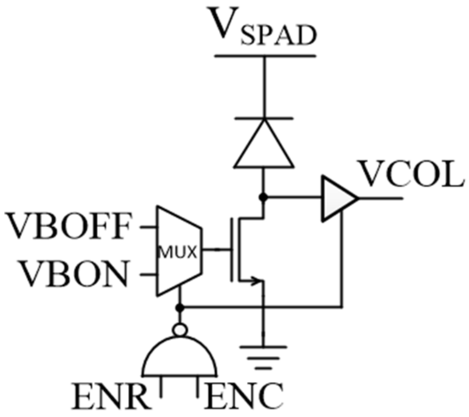

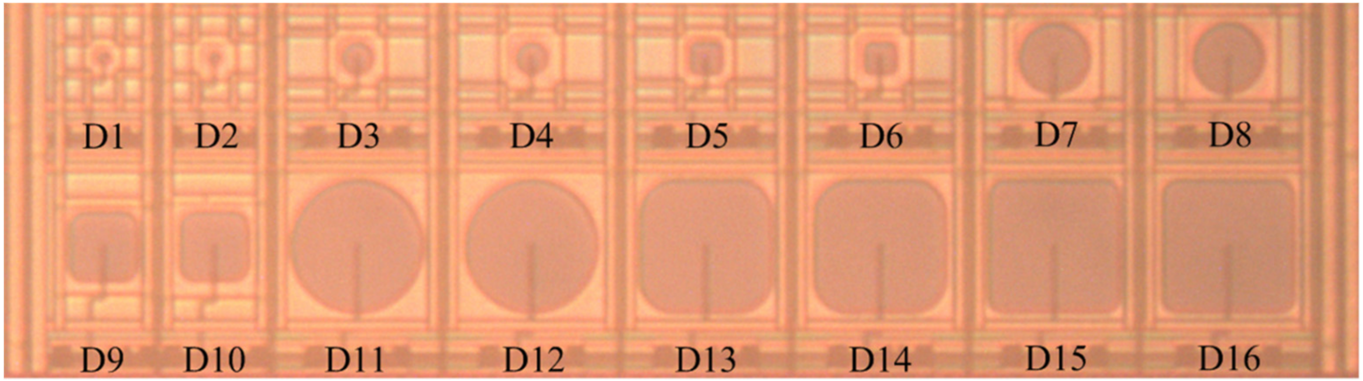

×6 test modules

Source: I. Vornicu et al., ESSDERC 2019

SPAD detectors for LiDAR: Breakdown voltage

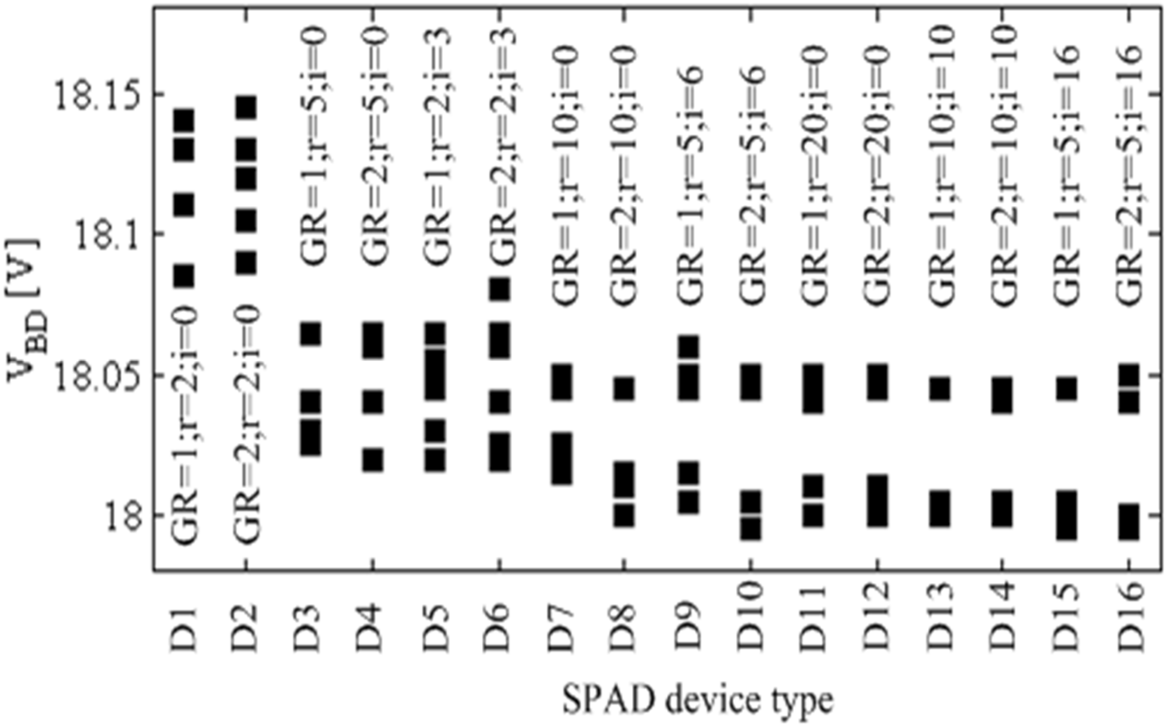

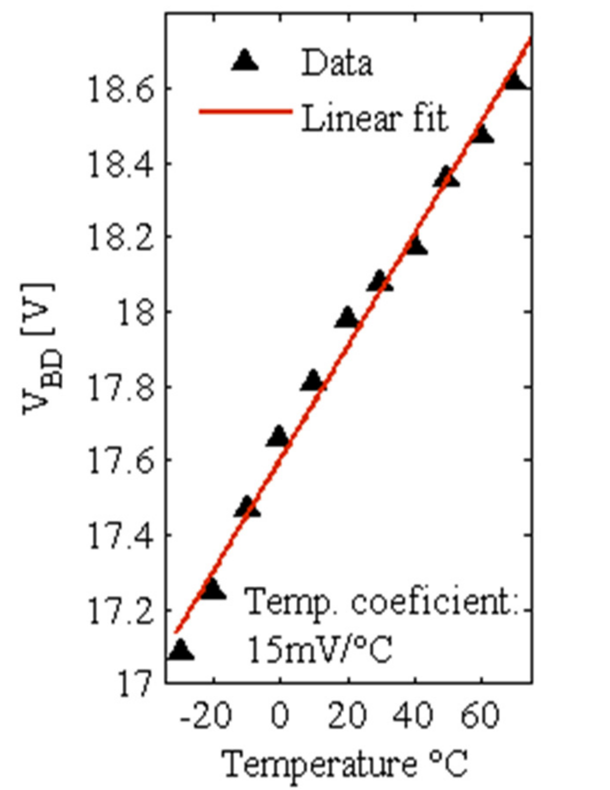

Active area Φ:
- D1-2: 3.7µm
- D3-6: 9.7µm
- D7-10: 22µm
- D11-16: 42µm

SPAD geometry
- Circular shape
  GR=1, 2µm
- Fermat shape
  GR=1, 2µm

SPAD detectors for LiDAR: Dark count rate (DCR)

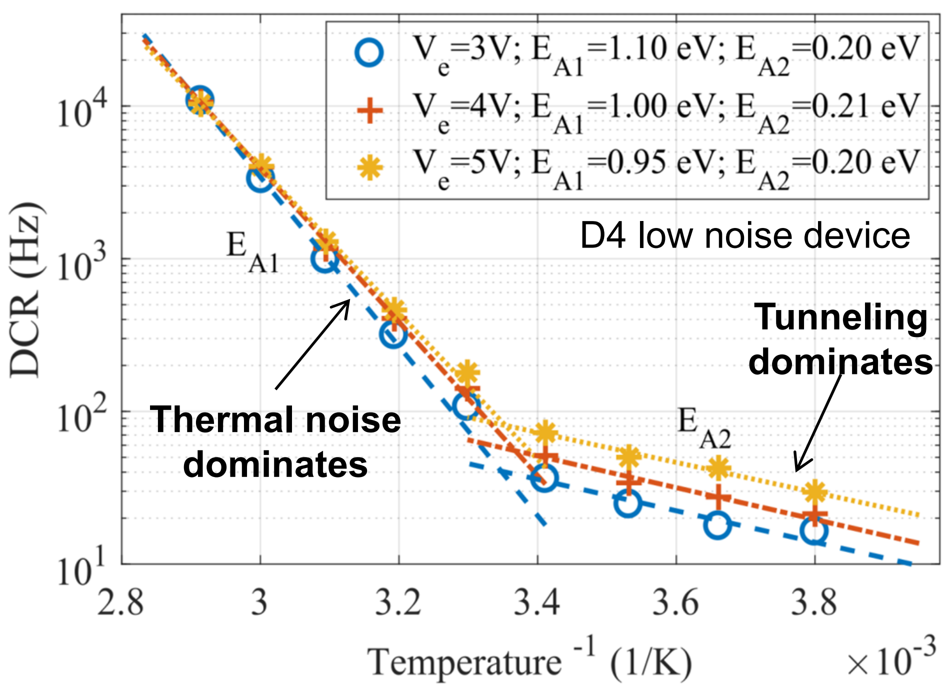

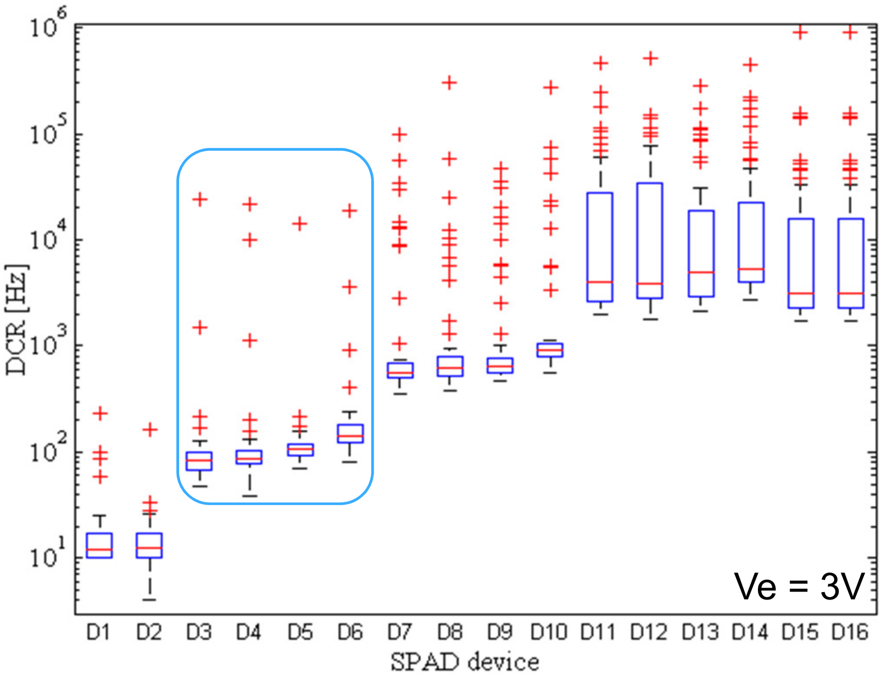

- Dashed line represent Arrhenius eq.:

$$DCR = Aexp\left(-\frac{E_A}{k_B T}\right)$$

- 10 chips, D1-D16 ×60 samples
- The large the active area, the larger the device–device deviation

SPAD detectors for LiDAR: Afterpulsing

- Measurement based on inter-avalanche histogram method:

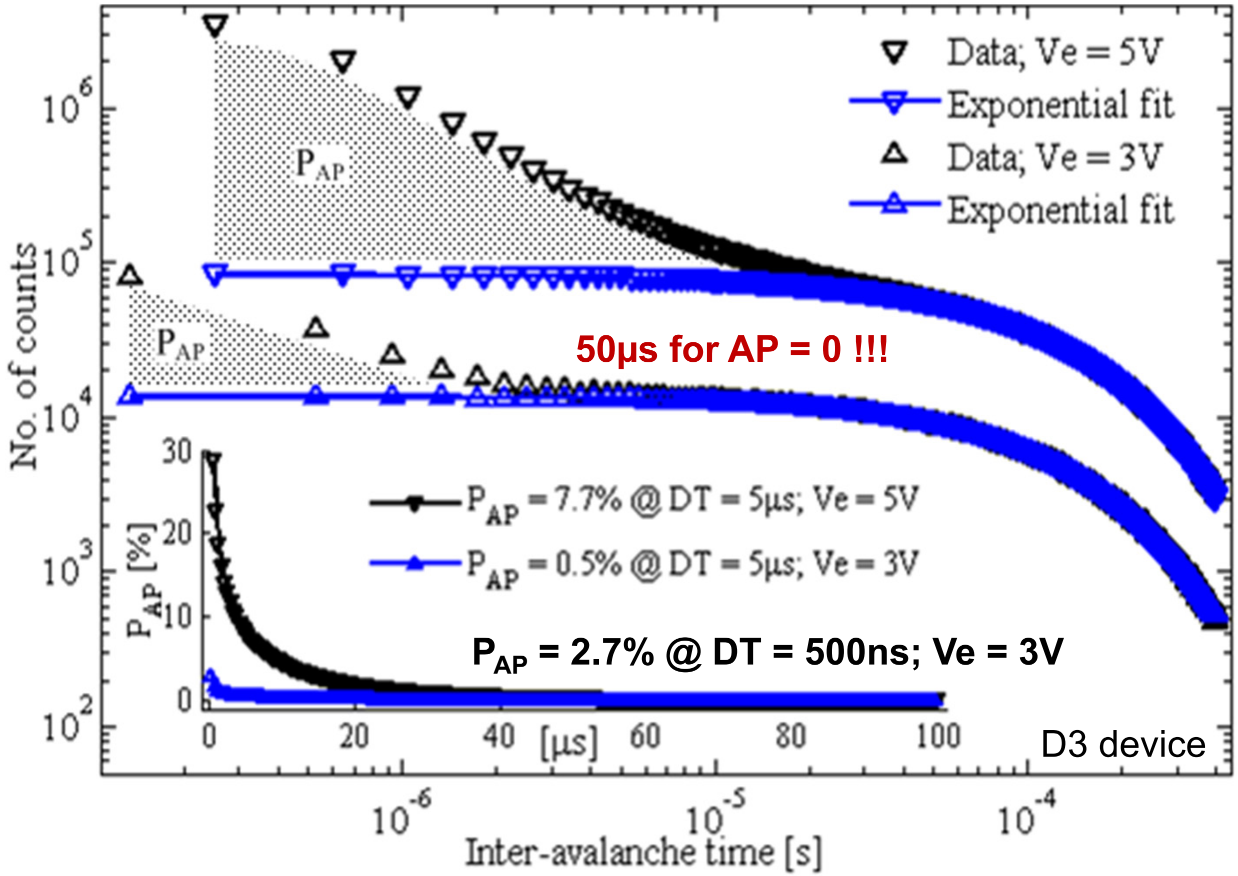

SPAD detectors for LiDAR: PDP

D3 device

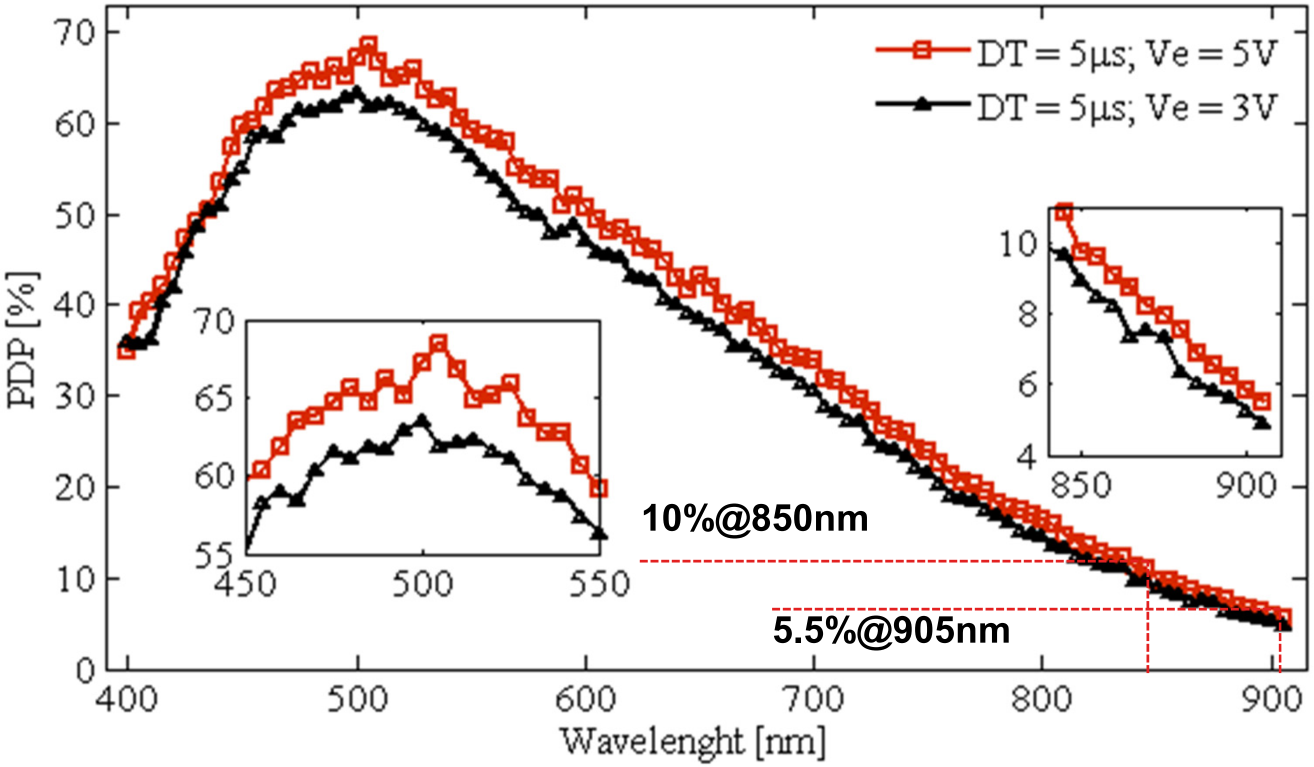

$$\mathrm{PDP} = \frac{\mathrm{TCR} - \mathrm{DCR}}{\mathrm{PhR}}(1 - P_{\mathrm{AP}})$$

→ Afterpulsing correction

SPAD detectors for LiDAR: Jitter

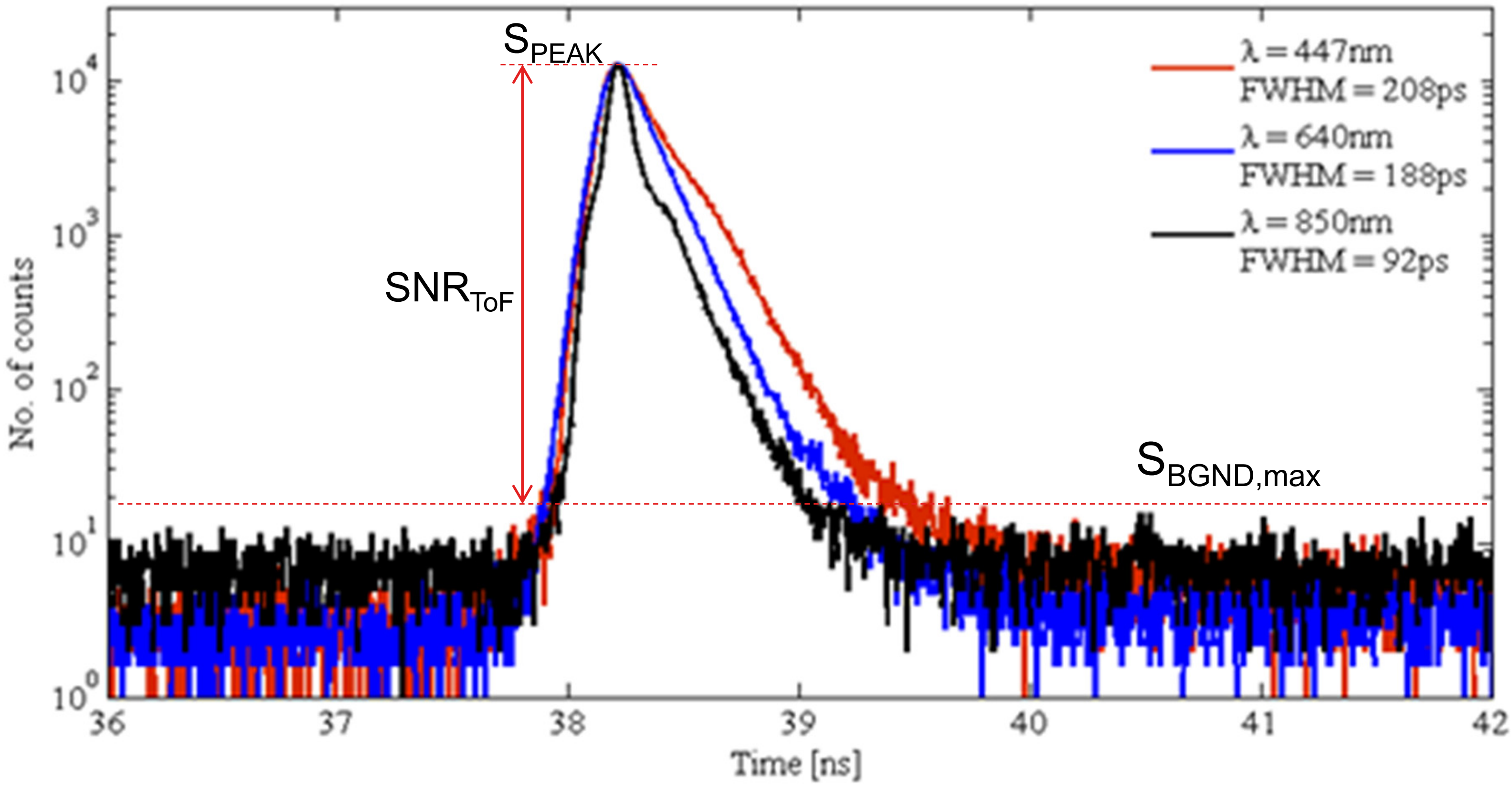

SPAD detectors for LiDAR: State-of-the-art comparison

IMSE-CNM

	Veerappan '16	Lindner '17	Xu '17	Moreno '18	Hutchings'19	This work
Tech. [nm]	180nm	65 CIS-BSI	150 CIS	110 CIS	65 CIS-BSI	110 CIS
SPAD	P-epi/BN(2)	PW/DNW	P+/NW	P+/LDNW(1)	PW/DNW	PW/DNW
V_{BD} [V]	25.5	12	18	20	12	18
Area [μm²] (ϕ)	113(12μm)	251(16μm)	97(10μm)	385(20μm)	9.18μm (pitch)	78(10μm)
Median DCR [Hz/μm²]	**0.3@3V**	**1.6@4.4V**	**0.4@3V**	**0.18@3V**	**0.23@1.5V**	**0.4@3V**
PDP peak [%] @ Ve, λ	33@3V, 480nm	30@4.4V, 660nm	27@3V, 450nm	52@6V, 455nm	28@1.5V, 615nm	64@3V, 500nm
PDP [%] @ 850nm	**9@12V**	**13@4.4V**	**7.5@5V**	**5@6V**	**15@3V**	**10@5V**
AP @ Ve, DT	7.2@11V, 300ns	0.08@4.4, 8ns	0.85@3V, 150ns	NA	0.4@NA	0.5@3V, 5μs
Jitter [ps] @ Ve, λ	**97@11V, 405nm**	**75 @ 4.4V, 700nm**	**42@4V, 831nm**	**80@4V, 831nm**	**70@2V, 773nm**	**92(3)@3V 850nm**

(1)P+/LDNW stands for P+/low doped NW; (2)P-epi/BN stands for P-epi/buried N; (3)It represents the total FHWM jitter

- C. Veerappan, E. Charbon, "A low dark count p-i-n diode based SPAD in CMOS technology", Trans. on Electron Devices, Vol. 63, No. 1, 2016.
- S. Lindner et al., "A high-PDE backside-illuminated SPAD in 65/40nm 3D IC CMOS pixel with cascoded passive quenching and active recharge", Electron Dev. Letters, Vol. 38, No. 11, pp. 1547-1550, Nov. 2017.
- H. Xu et al., "Design and characterization of a p+/n-well SPAD array in 150nm CMOS process", Opt. Express, Vol. 25, No. 11, May 2017.
- M. Moreno-Garcia et al., "Low-noise single photon avalanche diodes in a 110nm CIS technology", ESSDERC, pp. 94-97, Sept. 2018.
- S. W. Hutchings, "A Reconfigurable 3-D-Stacked SPAD Imager With In-Pixel Histogramming for Flash LIDAR or High-Speed Time-of-Flight Imaging, J. of Solid-State Circ., Vol. 54, No. 11, Nov 2019.
- I. Vornicu et al., "Low-Noise and High-Efficiency Near-IR SPADs in 110nm CIS Technology", ESSDERC, pp. 250-253, Sept. 2019.

Outlines

❶ LiDAR challenges

❷ Active illumination

❸ SPAD detectors

❹ **Noise suppression**

❺ Low power architecture

❻ ToF data processing

❼ Conclusions

Noise suppression

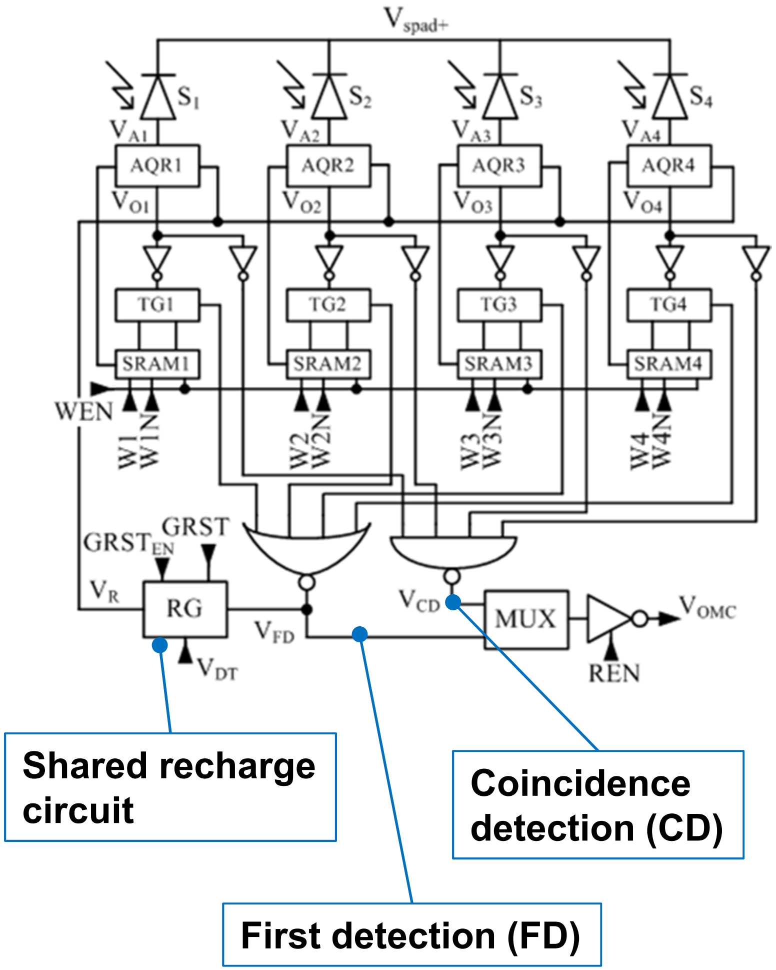

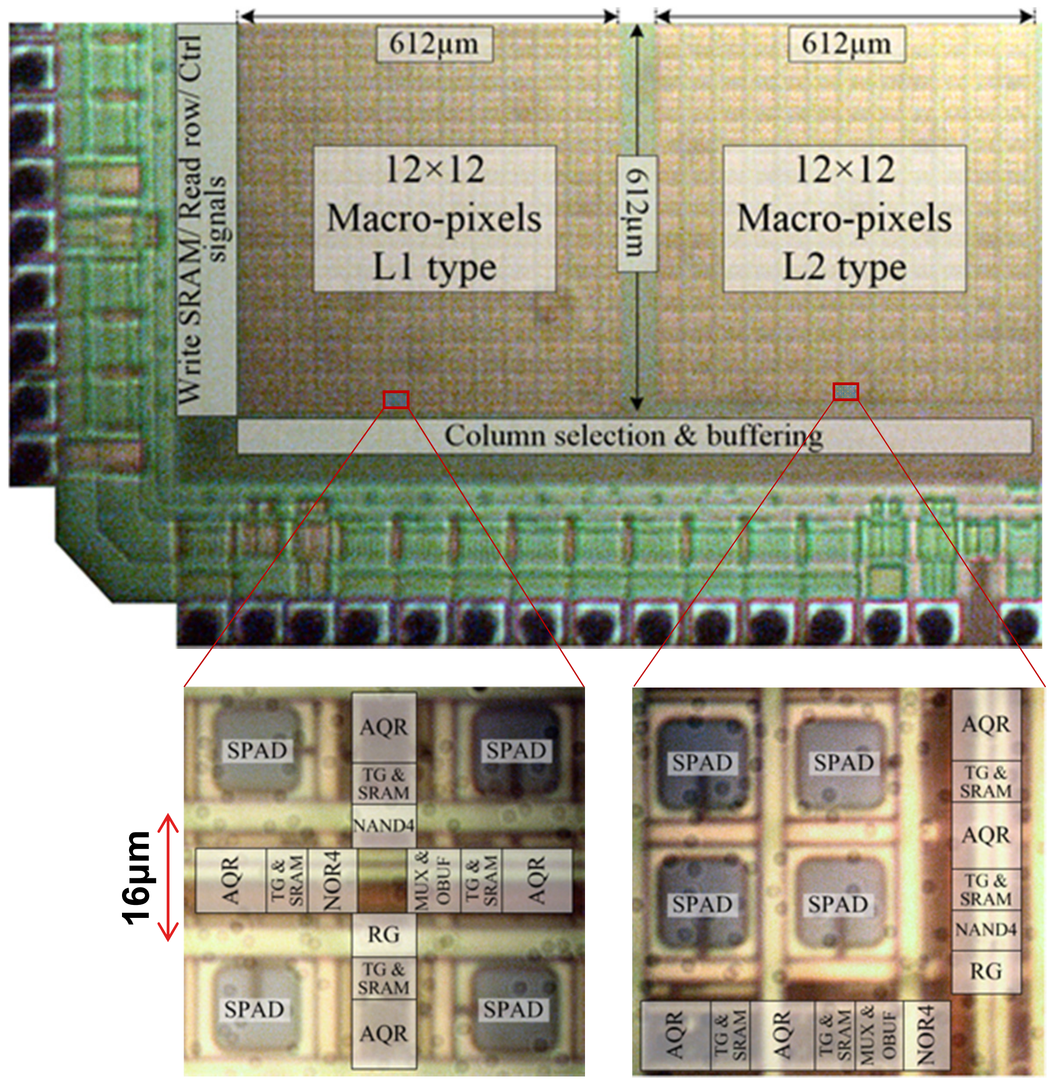

***Coincidence detection techniques:**

- M. Beer et al., "Background Light Rejection in SPAD-Based LiDAR Sensors by Adaptive Photon Coincidence Detection", Sensors, 18(12), 4338, 2018
- M. Perenzoni et al., "A 64×64-Pixels Digital Silicon Photomultiplier Direct TOF Sensor With 100-MPhotons/s/pixel Background Rejection and Imaging/Altimeter Mode With 0.14% Precision Up To 6 km for Spacecraft Navigation and Landing", J. of Solid-State Circuits, Vol. 52, No. 1, Jan. 2017

Noise suppression: DCR distribution

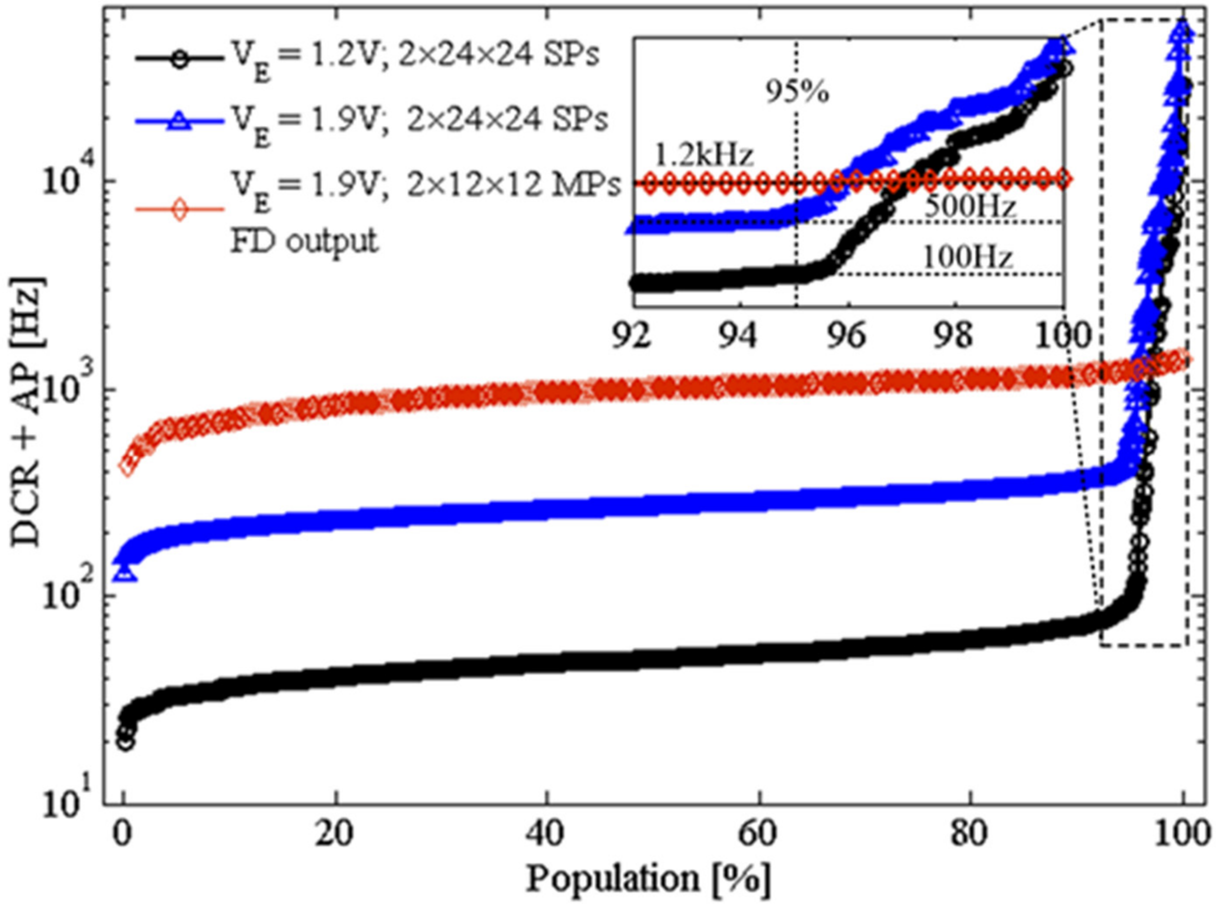

Total active area of macro-pixel: 420 μm^2

Noise suppression: Crosstalk

IMSE-CNM

$$\text{Crosstalk} = \frac{DCR_{w/} - DCR_{w/o}}{DCR_{hot}} \cdot 100$$

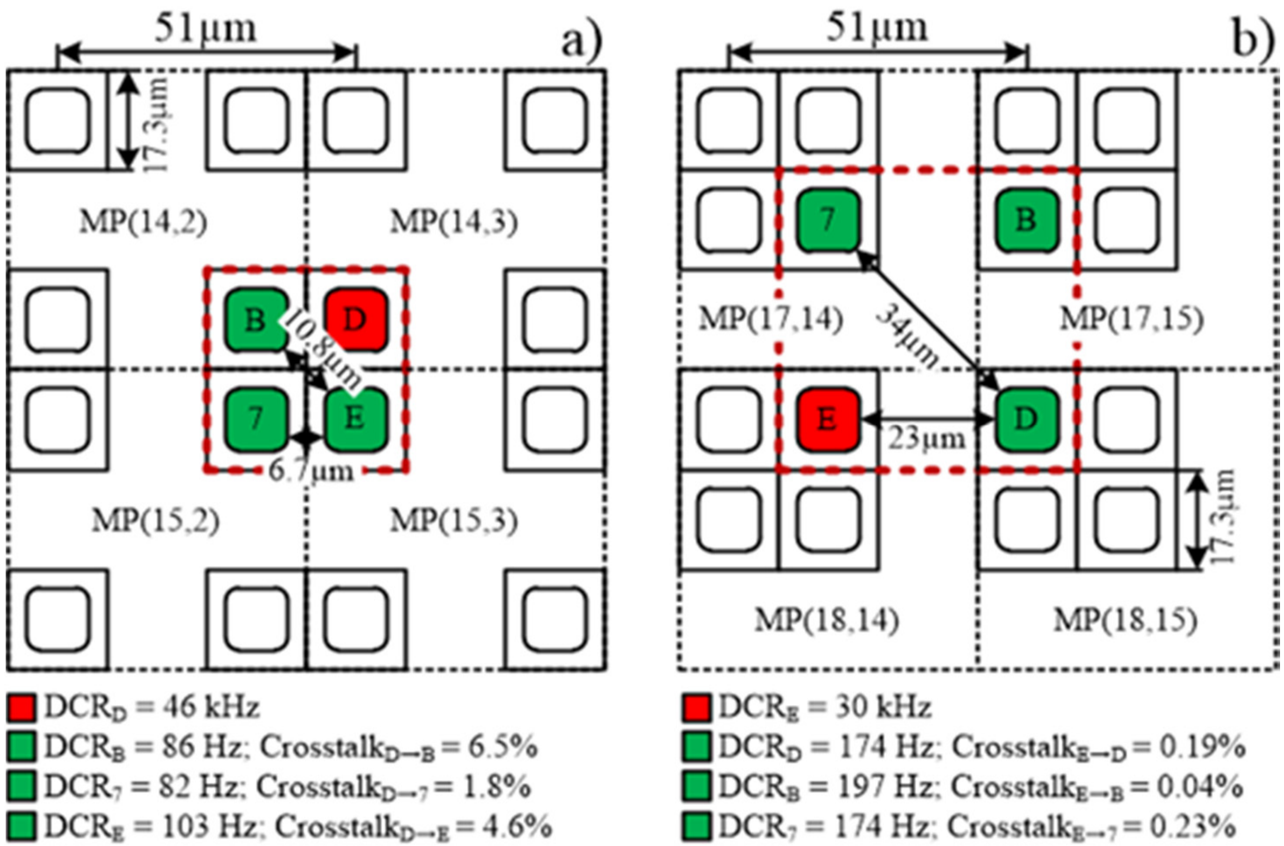

6.5% - same DNW   0.23% - DNWs separated @ 16µm

Noise suppression: ToF histogram noise floor

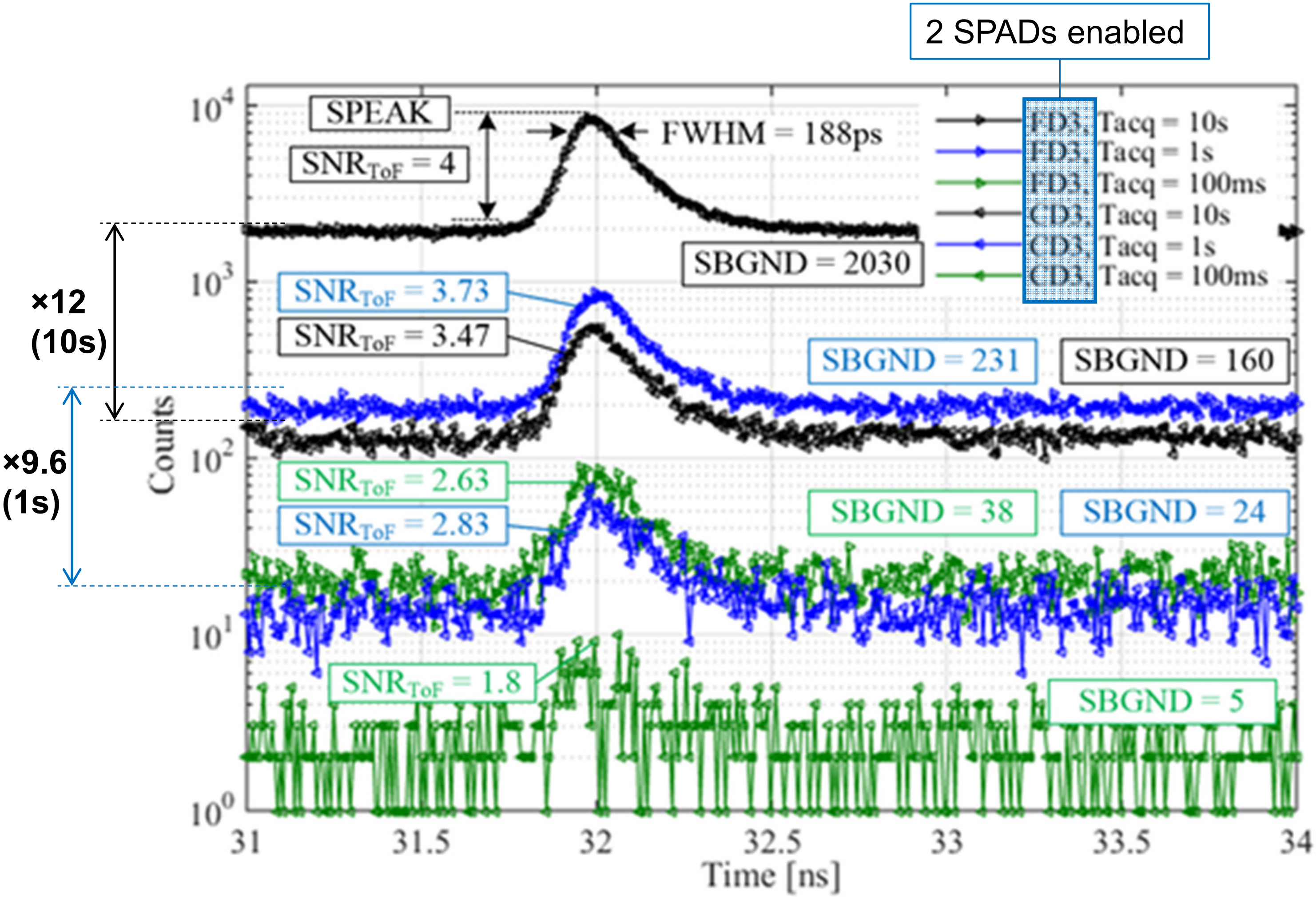

CD-2×SPADs; Tacq = 1s

- Background light: 162kcps
- Signal: 2.1kcps

FD-2×SPADs; Tacq = 1s

- Background light: 2.5Mcps
- Signal: 33kcps

- NO optical filter
- λ = 640nm
- CTW = 50ns

Noise suppression: Coincidence PDP

2 SPADs enabled (H&V)

2 SPADs enabled (diagonal)

3 SPADs enabled

4 SPADs enabled

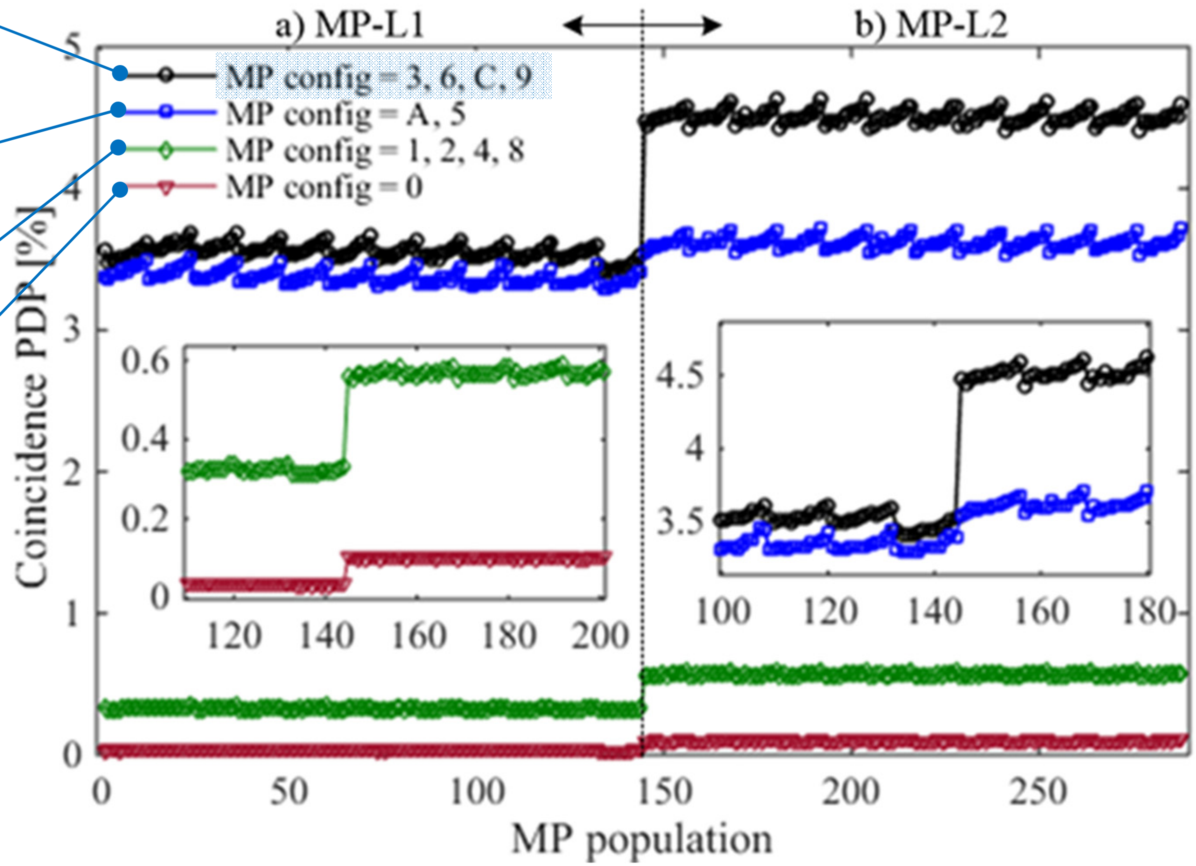

Coincidence detection @ 640nm, DT = 50ns

$$cPDP(DT,n) \sim \frac{PDP}{NSF(DT,n)}$$

Noise suppression: Depth map

4 SPADs in FD: Tacq = 1s

2 SPADs in CD: Tacq = 1s

4 SPADs in FD: Tacq = 100ms

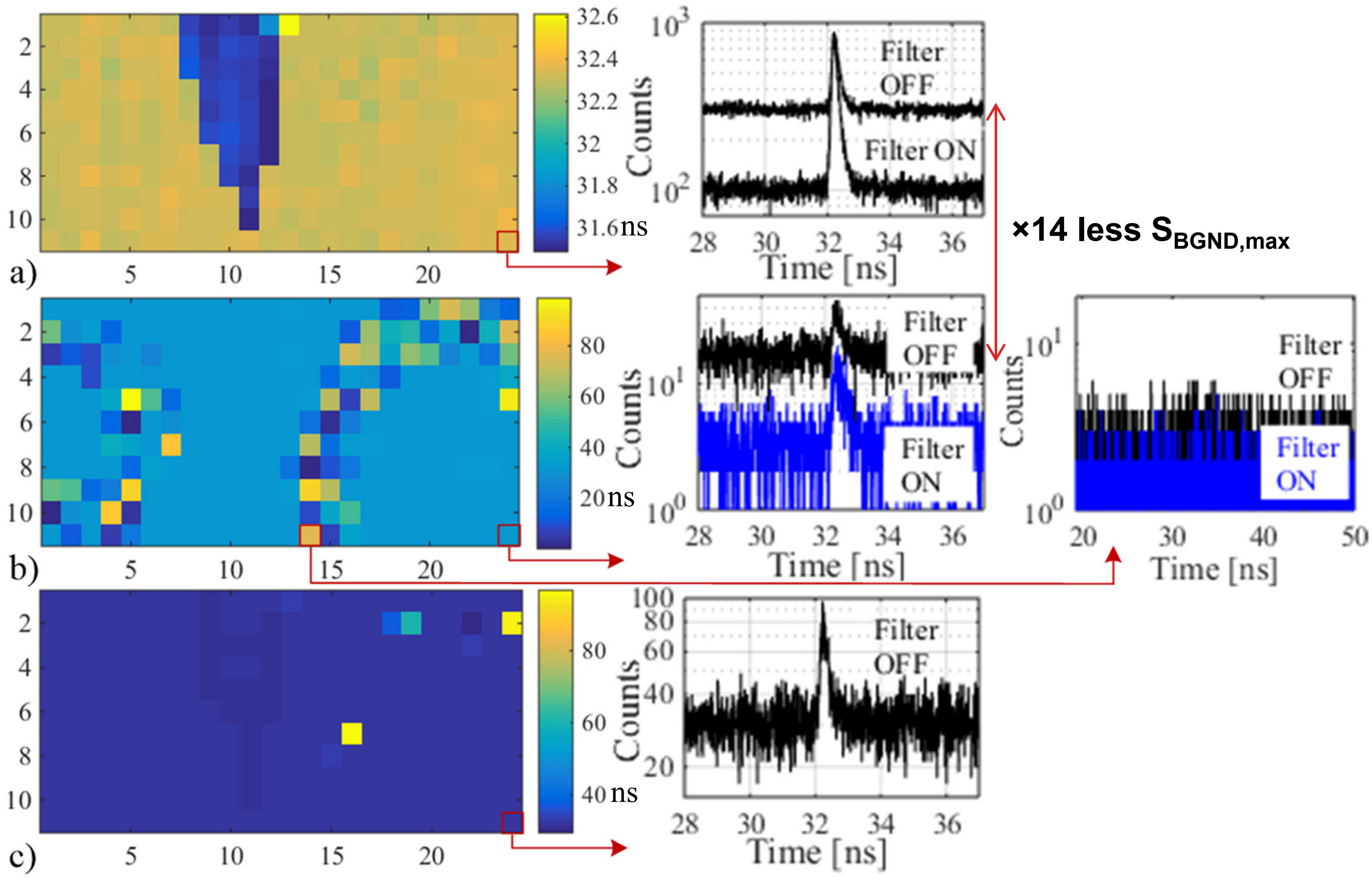

Experimental Setup:

- Signal = 0.4nW/mm2 @ 640nm
- BPF640nm OFF; Background = 3.8Mcps
- BPF640nm ON; Background = 1.4Mcps
- BPF640nm = ON/OFF
- Tbin = 8ps
- Flaser = 10MHz

Noise suppression: Intensity images (FD output)

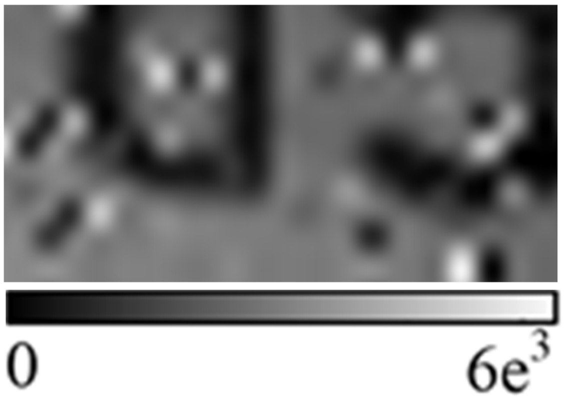

Tacq = 10ms;
1 SPAD activated

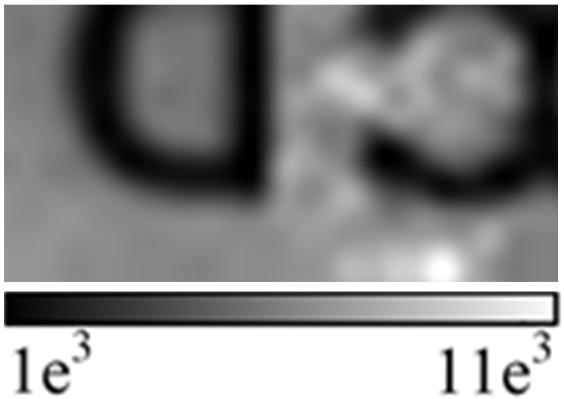

Tacq = 10ms;
2 SPADs activated

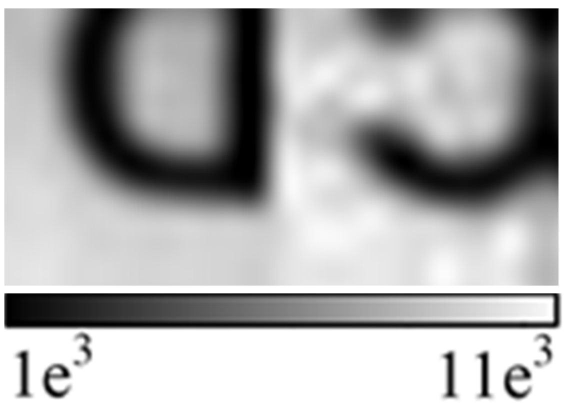

Tacq = 10ms;
3 SPADs activated

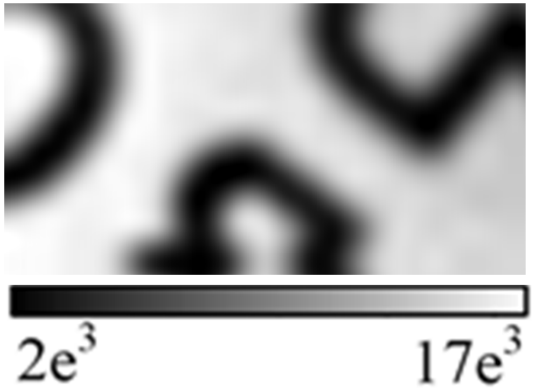

Tacq = 100ms;
4 SPADs activated

Outlines

Low power architecture

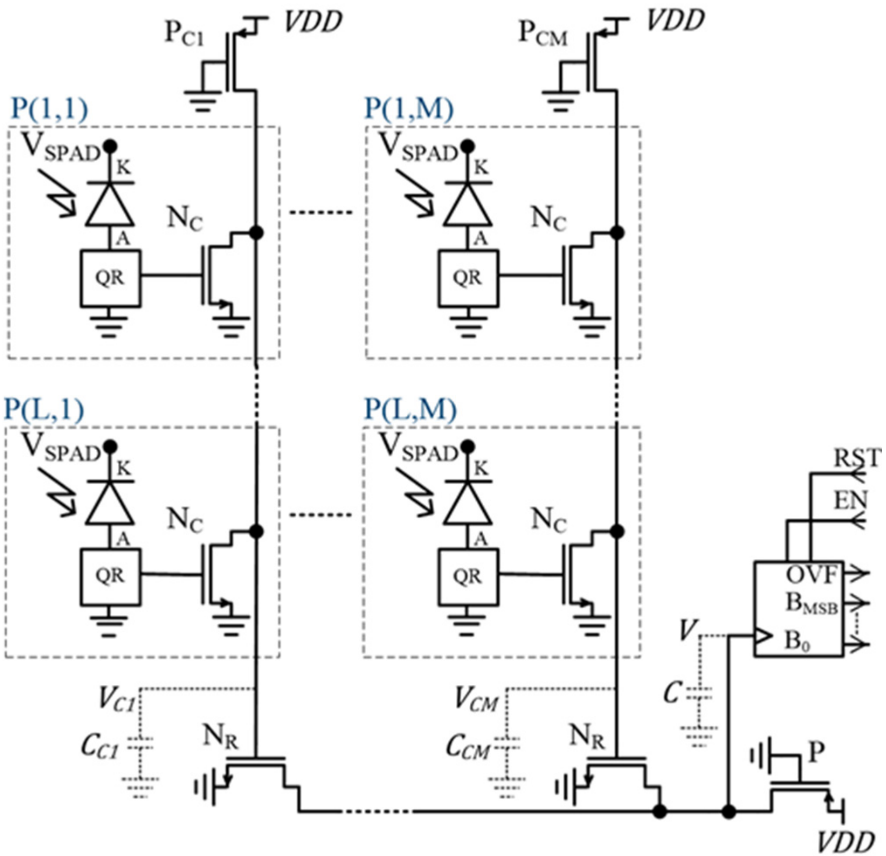

- Block diagram of conventional OR pulse-combining scheme

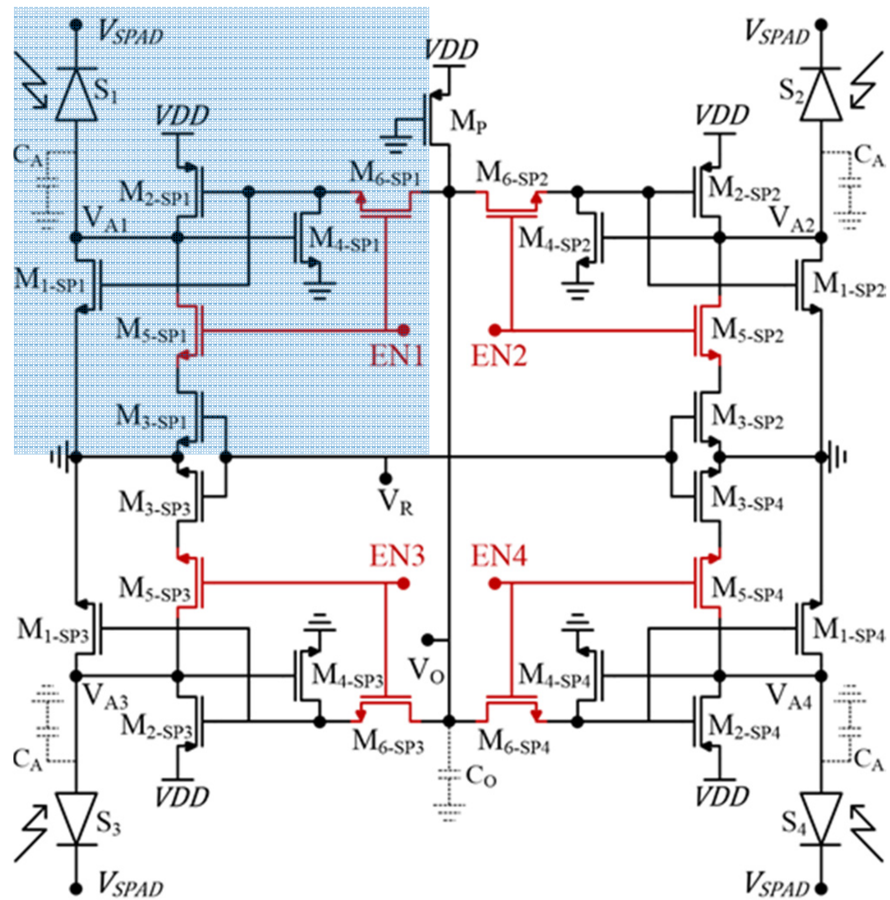

- Block diagram of the proposed macro-cell

Low power architecture: Uncorrelated light

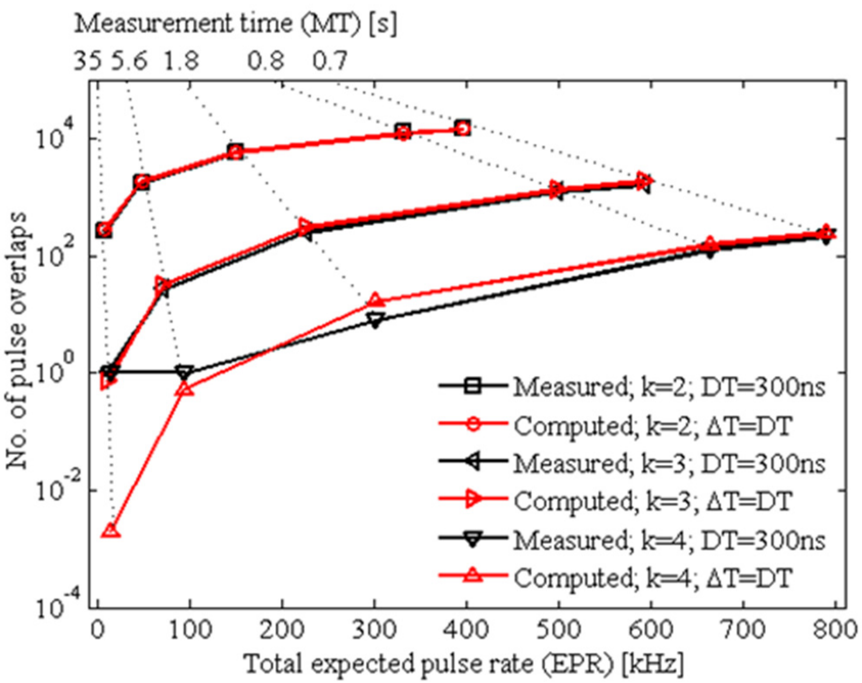

Pulse overlapping due to ***uncorrelated light***

$$P(k,\Delta T) = \frac{\left[\left(\sum_{n=1}^{k} EPR_n\right)\Delta T\right]^k}{k!} e^{-\left(\sum_{n=1}^{k} EPR_n\right)\Delta T}$$

$$No.of\ pulse\ overlaps = P(k,\Delta T)\frac{\mathrm{MT}}{\mathrm{DT}}$$

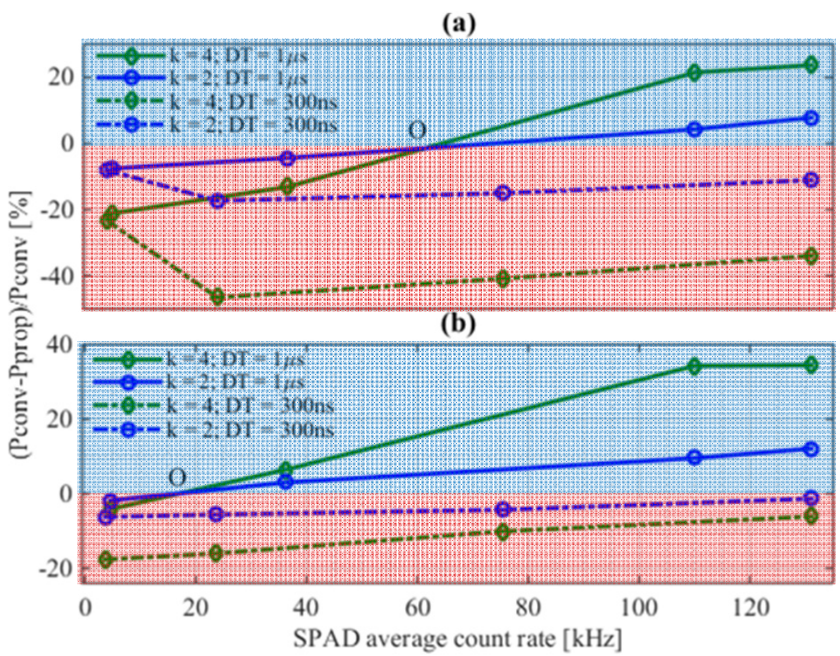

Power efficiency (PE) for ***uncorrelated light***; $M_{2\text{-}SCn}$ size is (a) $W/L = 2\mu m/360nm$; (b) $W/L = 600nm/1\mu m$

$$PE = \frac{P_{conv} - P_{prop}}{P_{conv}} * 100$$

Low power architecture: Correlated light

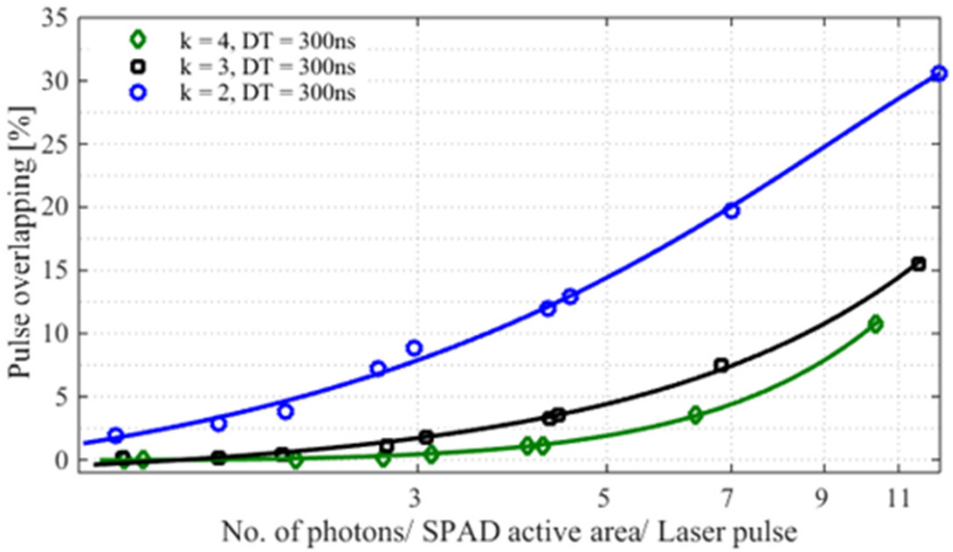

Pulse overlapping due to ***correlated light***

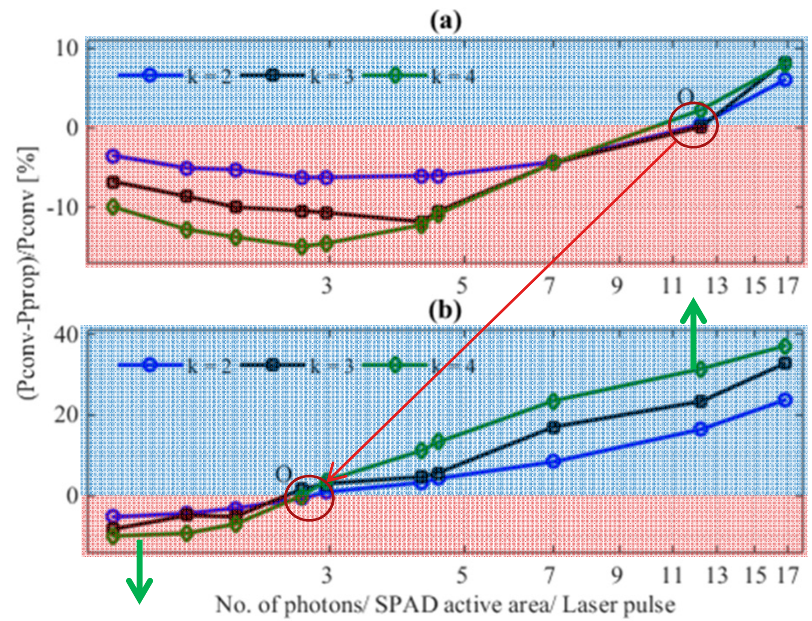

Power efficiency for ***correlated light***; $M_{2\text{-}SCn}$ size is (a) $W/L = 2\mu m/360nm$; (b) $W/L = 600nm/1\mu m$;

- ❑ DT = 300ns
- ❑ λ = 905nm
- ❑ PDP = 5%

Calibrate power efficiency according to expected input power

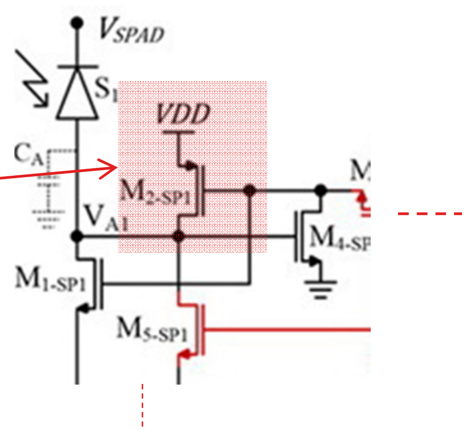

Outlines

1. LiDAR challenges
2. Active illumination
3. SPAD detectors
4. Noise suppression
5. Low power architecture
6. **ToF data processing**
7. Conclusions

ToF data processing: Gen1 SPADCAM @ IMSE-CNM

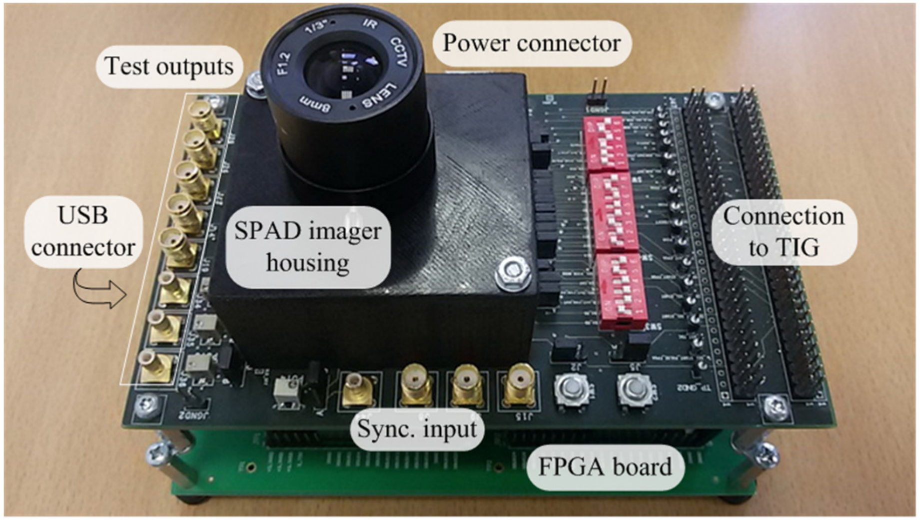

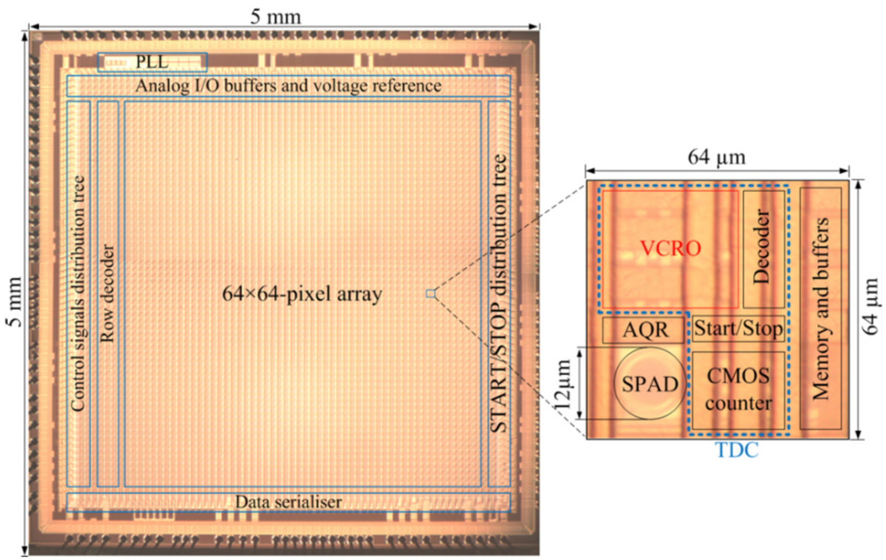

SPAD image sensor	CMOS technology	180nm-UMC
	Functionality	D-ToF/ Ph. Cnt.
	Shutter type	Global
	Format	64×64
	Fill factor	2.7%
	Output	Serial @ 50MHz
	Time gate (programmable)	2D – 87µs; 3D – 400ns

SPA D detector & AQR	Type	P+/N-WELL
	PDE @ λ	6.5%$^{(*)}$ @ 520nm
	Avg. DCR @ Ve	42kHz$^{(**)}$ @ 1V
	Dead time	5ns- 500ns
	Diameter	14µm
	Active area	113µm^2
	FWHM jitter	200ps
TDC	Type	In-pixel
	Architecture	VCRO-based
	Time resolution/Range	147ps/ 297ns
	No. of bits/ ENOB	11/ 9
	Area	1740µm^2
	INL/ DNL	3/ 0.55
	Conv. rate	500MHz

Source: i) US-CSIC IMSE CVIS Lab @ I. Vornicu et al. *IEEE ISCAS*, 2017
ii) US-CSIC IMSE CVIS Lab @ I. Vornicu et al. *IEEE TCAS-I, 2017*

ToF data processing: FPGA based ToF histogramming

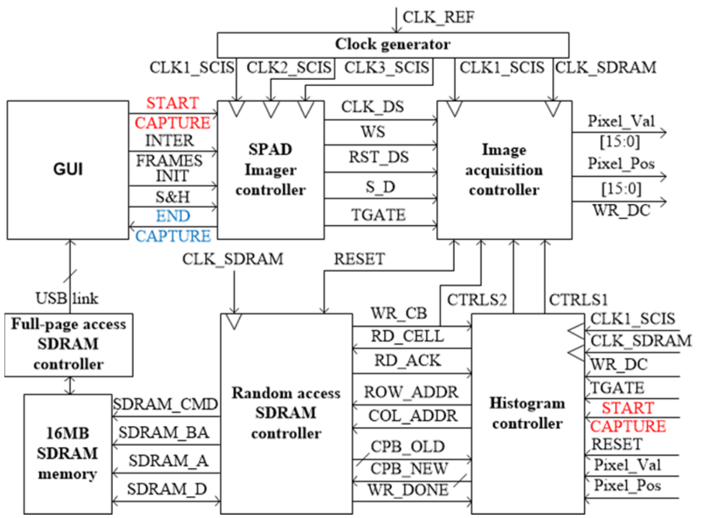

@1000 fps

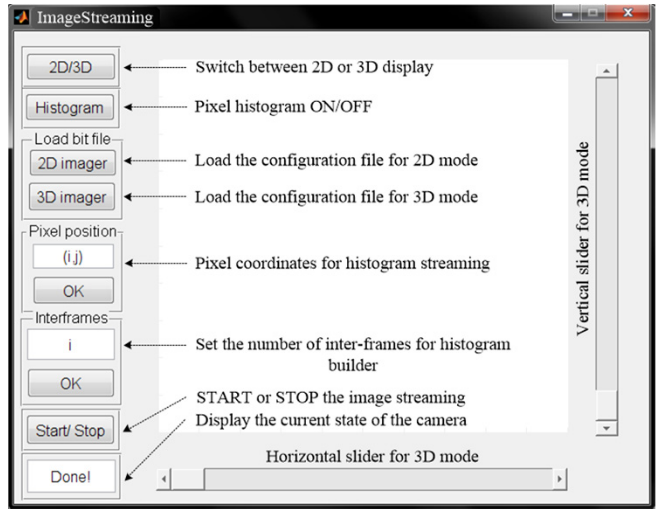

SPADCAM GUI

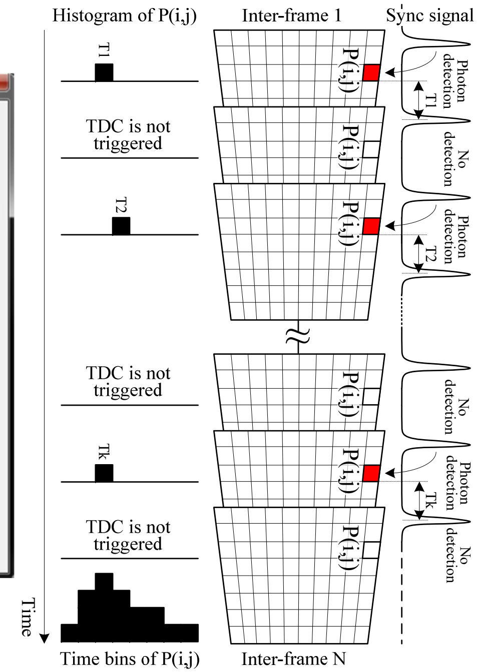

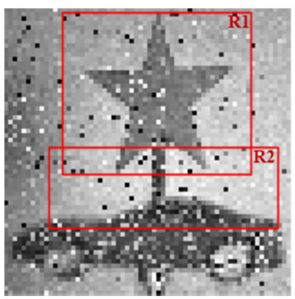

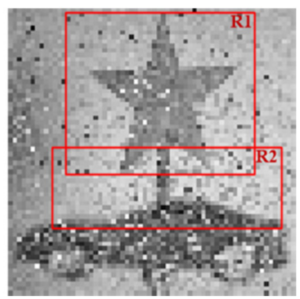

Histogram requirements

Memory size:

11 bits pixel → 2048 bins
10 bits of bin depth
64×64 histograms

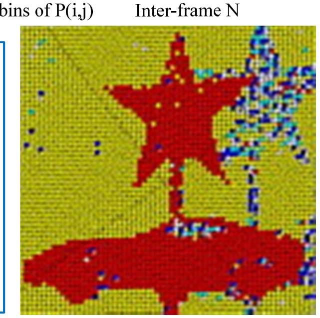

- **Sensor using standard CMOS Technology:**
  - **high DCR;**
  - **low PDE**

Complete histogram requires:

80Mb for only 4kpixels on 11bits
1.25Gb for only 4kpixels on 15bits

Source: US-CSIC IMSE CVIS Lab @ *IEEE Sensor J, 2017*

ToF data processing: Hardware histograms compression (1)

ToF histogram features:

- Memory footprint scales with 2^N, N = number of bits
- ToF information is located on a small fraction of bins

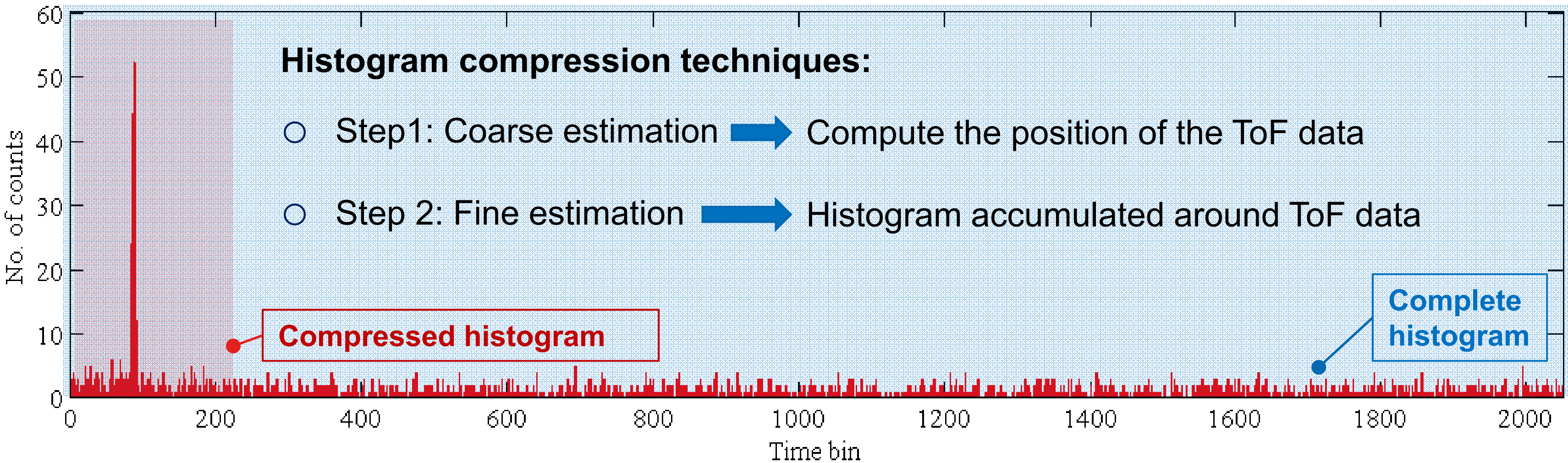

Challenges

- Large compression rate
- Unaltered frame rate
- Free of uncertainty errors

***Histogram compression techniques:**

- A. Sharma et al., *Patent US 2017/52 A1*, Apple Inc., Cupertino, CA (US)
- A. Erdogan et al., *Patent WO 2018/122560 A1*, University of Edinburgh (GB)
- I. Vornicu et al. *IEEE Sensors J.,* Vol. 19, No. 6, *March 2019*;
- C. Zhang et al. *IEEE J. of Solid-State Circ.*, Vol. 54, No. 4, *April 2019*

ToF data processing: Hardware histograms compression (2)

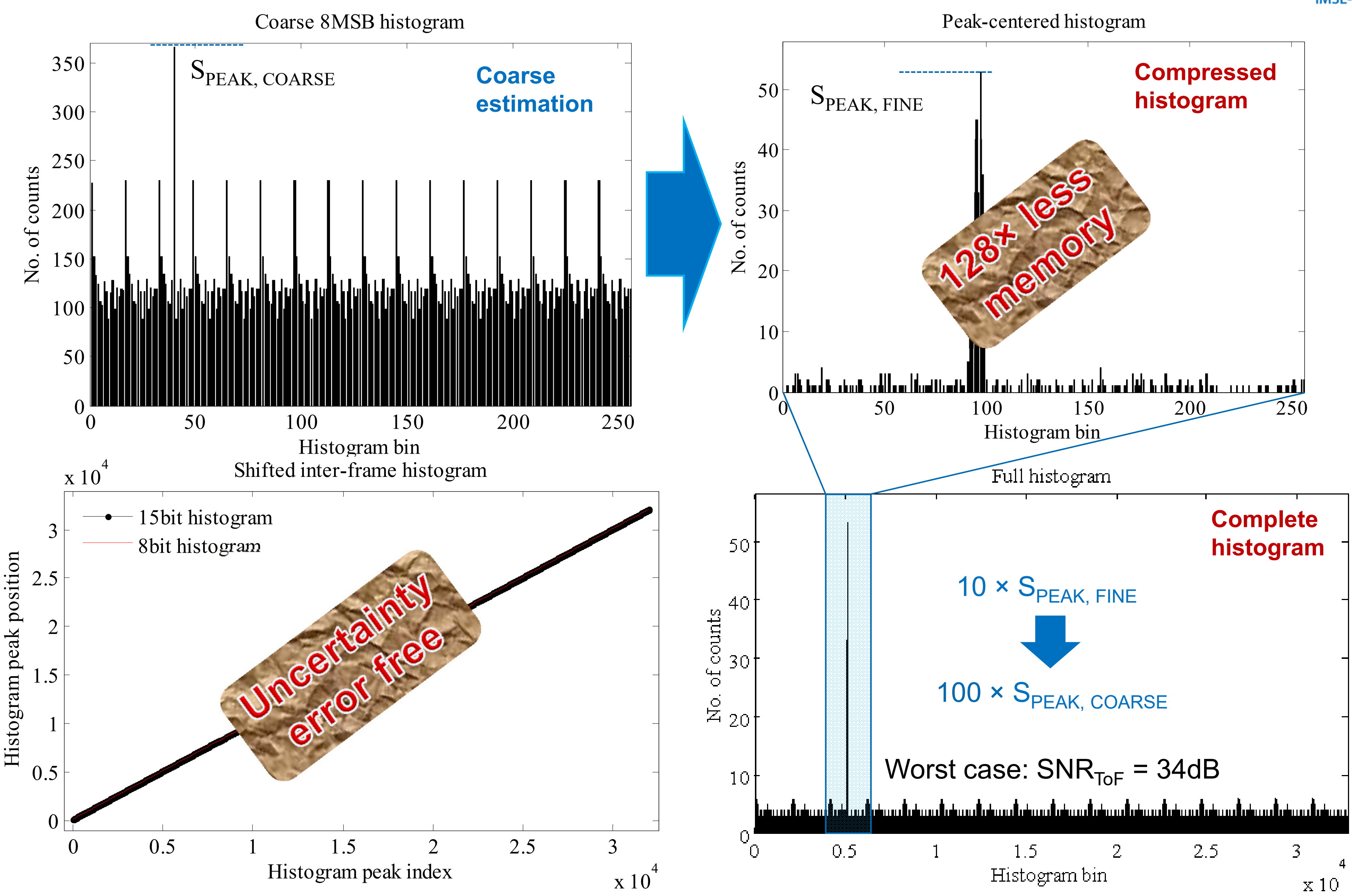

Outlines

Conclusions

- Active illumination
  - Compliant with eye safety standards
  - Shorter laser pulses combined with scanning
  - Temperature stability with higher duty cycle
  - Selectable VCSEL arrays
- SPAD detector
  - High PDP most wanted @ laser wavelength
  - CD improves noise floor but affects cPDP as well
  - Sharing recharge circuits improve FF, holding the advantages of active quenching recharge approach
- Sensor architecture
  - Smart OR combining scheme may save power
  - Adapted to the illumination setup
- On-chip ToF processing
  - Data throughput challenge
  - Histogram compression by centering the acquisition around the ToF data

Acknowledgment

This work has been funded by the Office of Naval Research (USA) ONR, grant No. N00014-19-1-2156 and by the Spanish Ministry of Economic Affairs and Digital Transformation (MINECO)

Thanks for your attention !